Optics and Photonics Research for Montana Economic Development - MREDI Project
Quarter 5 Report – Nov. 9, 2016

Joseph A. Shaw, Principal Investigator (joseph.shaw@montana.edu)

Introduction
This project is on schedule and within budget, and is continuing to enable important collaboration between the optics and photonics research and business communities. In the following pages we report specific progress toward meeting the milestones for each subproject.

On 27 September 2016, participants gave a demonstration of the project to visiting legislators and other political and business leaders from around the state. The optics and photonics project demonstration participants included 7 faculty, 3 research scientists or engineers, 9 students, and 11 representatives of 7 local optics and photonics companies. The result was a lively, informative discussion between the visitors and project faculty, students, and business partners. Posters and hands-on hardware demos were shown for each subproject contained within the overall “Optics and Photonics Research for Montana Economic Development” project. Figure 0-1 is a photograph of this successful event.

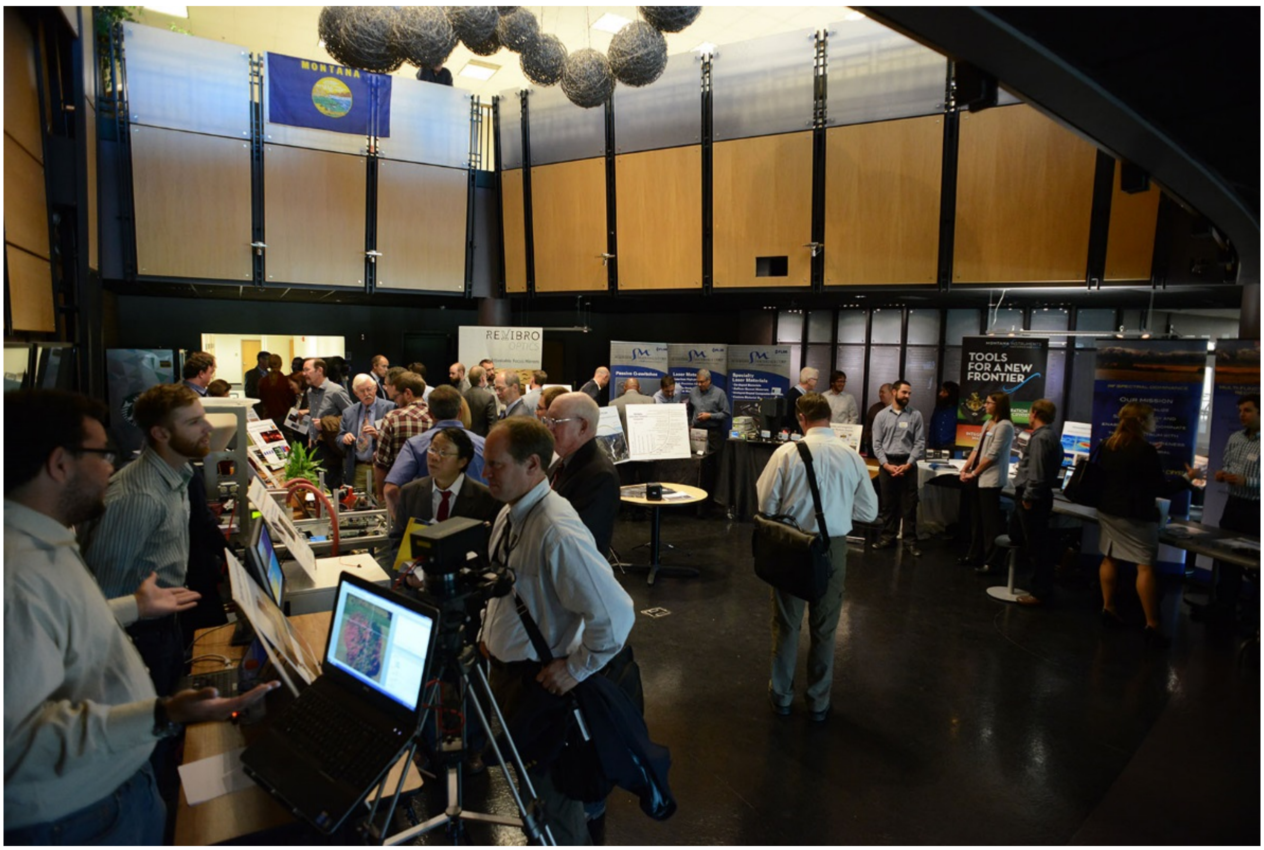

Figure 0-1. Photograph of the Optics and Photonics MREDI project demonstration to political and business leaders at the MSU-Bozeman campus on 27 September 2016.

Subproject 1: Ultra-compact spectral imagers for precision agriculture and mapping of wildfires and natural resources (Joseph Shaw, joseph.shaw@montana.edu, with NWB Sensors, Inc.). Development of ultra-compact imaging systems for weed mapping in precision agriculture, UAV mapping of wildfires, and a wide variety of ground-based and airborne remote sensing.

Milestones

a) September 30, 2015: Initial agricultural data collection completed
b) December 31, 2015: Initial weed maps complete
c) June 30, 2016: Prepare a refined imaging system and application-specific algorithm
d) December 31, 2016: Complete results of summer 2016 harvest experiment
e) June 30, 2017: Finish imaging system and algorithms and transfer to private partner

Introduction

Our fifth-quarter activities have been focused on finalizing the image collection from Montana fields during harvest and begin processing those images to create weed maps. During this quarter we deployed imaging systems on combines during harvest of approximately 1700 acres in 18 fields in Montana. We used support vector machines (SVM) to process the data and create weed maps. We have optimized algorithms to provide faster data processing times and improved the accuracy of our SVMs by performing other optimized image processing techniques. We are presently in the midst of a quantitative analysis of the accuracy of the weed-mapping process.

Weed mapping

Data Collection Summary

We captured approximately 270,000 images during the summer 2016 harvest. These images were collected over 11 days in the field. We had a total of 11 cameras deployed, while working with 7 different growers in Fairfield and Churchill, Montana. All of the data have been backed up and analyzed for accuracy. During this year's data collection, we were able to map complete fields with multiple growers, which was very important to begin determining how accurate our weed mapping algorithms are when applied to entire fields. Table 1-1 shows the total data collection for each type of camera used in the field.

Figure 1-1 is a photograph showing how the imaging systems were mounted in the combine during data collection. There were 5 different cameras mounted in this particular combine: two customized visible and near infrared Raspberry pi cameras, two versions of a commercial visible-light GoPro camera, and a commercial visible-light Garmin VIRB. The Garmin camera is a commercial "action camera" similar to the GoPro, but with an accurate on-board GPS used for geotagging the images. The project initially began with custom-designed visible and near-infrared cameras, but in summer 2016 we also extensively tested the capabilities of commercial-off-the-shelf video cameras that do not require custom filters or optical components. We tested the stationary GPS stray of the VIRB before going into the field and found it was well within our accuracy requirements needed for weed mapping.

Table 1-1. Data collection summary for summer 2016.

Date	Cameras			
	Garmin	Pi RGB	Pi NIR	GoPro
7/26/2016	10090	0	0	0
8/11/2016	23931	0	0	0
8/12/2016	2060	1464	1464	5568
8/13/2016	9095	8869	8869	6097
8/14/2016	13223	6453	6453	0
8/15/2016	14530	5225	5225	5096
8/16/2016	40278	7509	7509	3920
8/17/2016	26956	6988	6988	4220
8/23/2016	15338	0	0	0
8/24/2016	11172	0	0	0
8/31/2016	2186	0	0	0
Totals:	168859	36508	36508	24901
Total # images:	266776			

Figure 1-1. Imaging systems mounted inside the combine cab with 5 different cameras.

Field Mapping

Once we completed the field experiments to collect images, we began processing and creating maps from the 2016 data. Currently we are ahead of our quarterly milestone goals in terms of data processing. The 2016 data have all been processed using an existing support vector machine (SVM) that was developed last year.

Figure 1.2 shows weed maps from the same field in 2015 and 2016. The map from 2015 shows weeds detected in the GoPro images using the SVM-trained GoPro data set. The GPS accuracy was improved on the GoPro this year from the 2015 imagery by using a high powered antenna that decreased GPS stray in its geotagged images. The map from 2016 shows weeds detected in the Garmin VIRB images, which were also processed using the same SVM used by the GoPro images. These images suggest that this particular field had fewer weeds during the 2016 harvest because Initial detection results were similar in both the GoPro and Garmin imagery. We presently are conducting calculations and experiments to verify the results and quantity the statistical uncertainties of the weed maps (to be reported later).

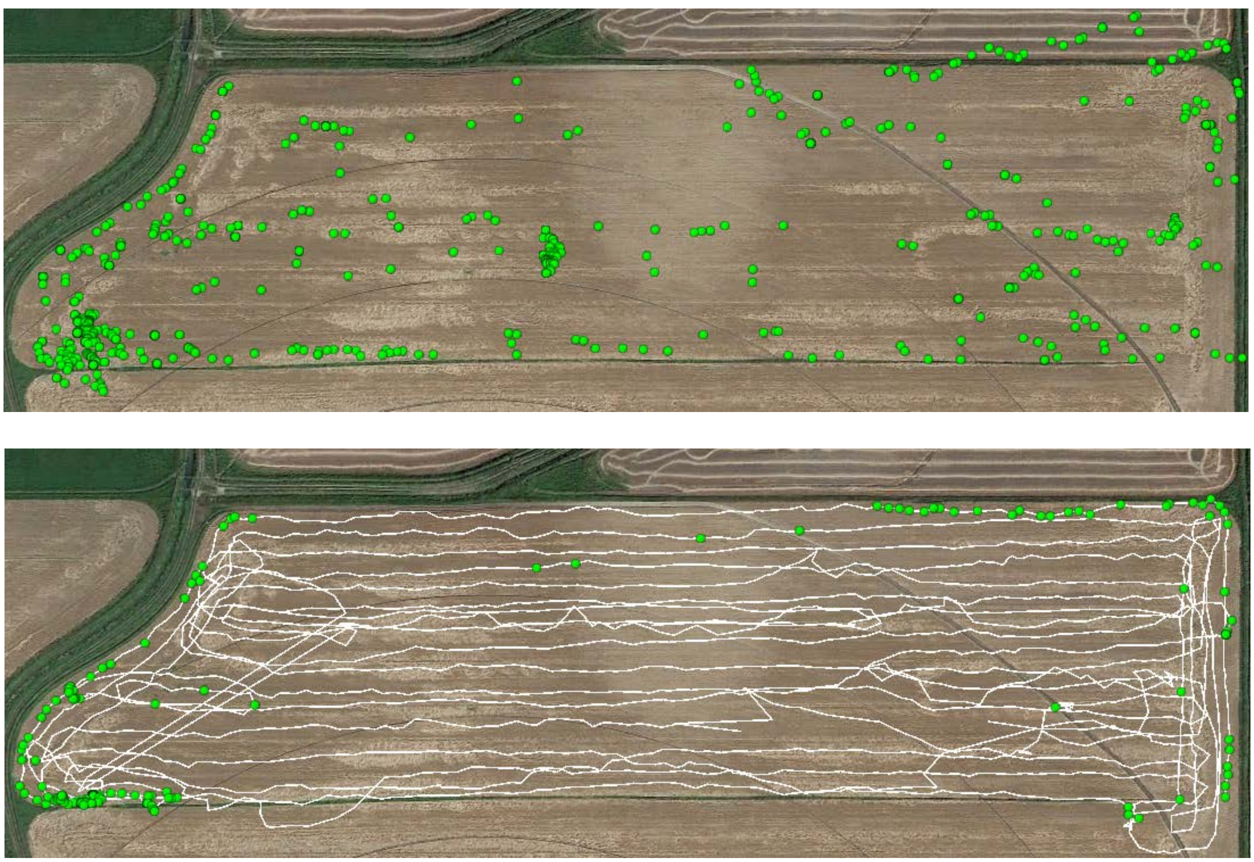

Figure 1-2. Weed maps from 2015 (GoPro top) and 2016 (VIRB bottom) using two different RGB cameras.

Figure 1.3 shows the extensive area on which we collected data during the 2016 harvest in Fairfield, MT. We were able to map several entire fields that total approximately 1200 acres during this year's data collection. The sections of land shown in the image are from four different farmers, who all expressed high interest in the application of our weed mapping imaging systems.

Figure 1-3. Regions of data collection in Fairfield, MT, during the 2016 harvest.

New Species of Crops and Weeds

We also collected images during summer 2016 from fields containing lentils, garbanzo beans, and dried peas (Fig. 1.4). The ground coverage of these new crops was slightly different in comparison to the wheat and barley fields, but we expect to see similarly successful weed detection results with these new crops. We were able to identify at least 10 new weed species in our imagery, which we hope to identify and distinguish from each other. To aid in this process, we also collected spectral reflectance data from each weed and plant species. We will explore the use of these spectral reflectance data to refine our machine learning algorithms and improve the accuracy of the weed maps.

Figure 1-4. New imagery of Chickpeas (Left) and various weed species (right) collected.

Image Processing Algorithms

Our existing SVM uses an assortment of GoPro images collected during the 2015 harvest. Using this SVM appears to be successful also for detecting weeds with the Garmin visible-light camera. However, a next step will be to begin training a new SVM to process the Garmin VIRB images. This will require a diverse new set of images that accurately define all objects seen in the imagery. Example processed images are shown in Figure 1.6 for the two visible-light cameras.

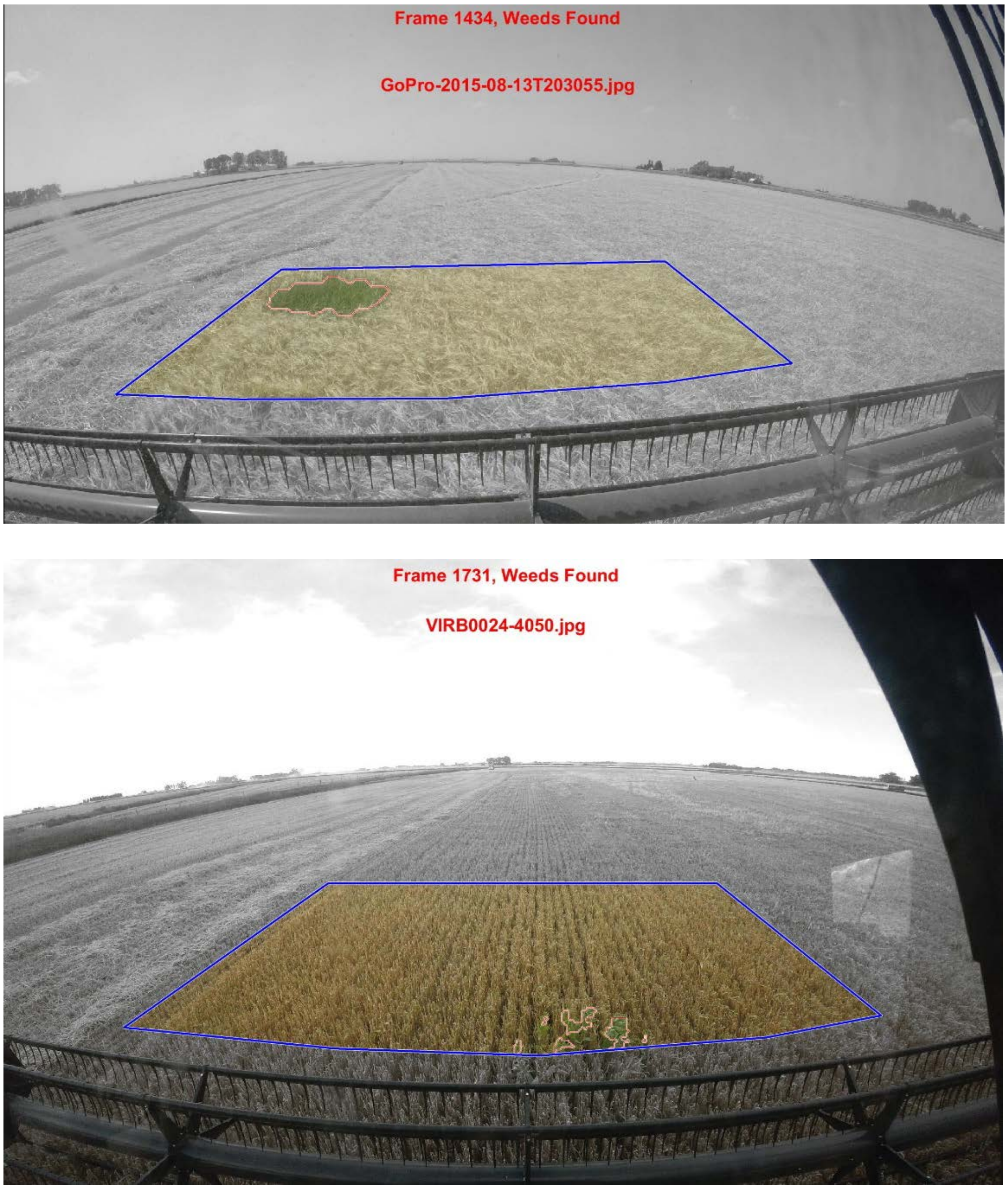

Figure 1-5. Processed imagery from the 2015 and 2016 harvest experiments using two different RGB cameras.

To test the accuracy of our weed detection algorithm in an unbiased method, we needed to develop a process to analyze the detection results. Using the data collected in one field from two consecutive years, we processed images into a user-friendly time-lapse video. This video is being used by a group of people to visually determine when the automated algorithm is detecting weeds correctly, detecting false positives, or missing weeds. We will compare viewer results with our machine learning results and then compare those results to the expert results. During the next quarter we will perform a statistical analysis on the viewer, machine, and expert detection-rate data to quantify how well our current weed detection algorithms are working.

New Data Processing Techniques

We also developed new data processing techniques to improve the accuracy of our weed detection algorithms. For example, uneven ground we encountered in Churchill, MT caused the orientation of the camera field of view to change considerably throughout the harvest. The software originally tried to look for weeds in the sky region of these images, so we developed a horizon-detection algorithm that analyzes where the sky line in an image to the desired region our data processing needs to take place. Correcting for the uneven horizon in the images will give us information on how we adjust our processing masks (an example is shown in Figure 1.6). These images could not be processed unless we implemented a method to correct for the uneven ground.

We also developed a color correction algorithm for correcting lighting and color tone values in images. We ran into an issue of incorrect brightness and color adjustments on the VIRB cameras, which is why we need to analyze and correct each image individually to provide a consistent data set. The color correction algorithm will hopefully improve the accuracy of our SVM by correcting the brightness in the images when it is cloudy or dark out. We collected data during the night in a few occasions which we intend on analyzing using a similar method.

Figure 1-6. Image processing for horizon detection used in mask adjustment of hill imagery.

Dissemination of information

We presented a poster and live demonstration of low-cost agricultural imaging systems during the 27 September 2016 tour by political and business leaders. Additionally, at the 4 October 2016 annual conference of the MSU Optical Technology Center, an oral presentation on this work was given by MSU graduate and Research Engineer Seth Laurie. Two scientific publications are presently in progress.

Expenditures to date (Grant 41W410) Personnel $123,688.88., Benefits $31,887.93., Operations $32,744.54., Sub Award $93,652.99, total Expenditures **$281,974.34**

Subproject 2: High-performance, real-time image processing for hyperspectral imaging (Ross Snider, rksnider@ece.montana.edu with Resonon, Inc.) Design a high-speed hyperspectral waterfall sorting system to fuse object edge information with hyperspectral data to sort agricultural products quickly and efficiently using Resonon's Hyperspectral Imagers and remove rejected items via air jets. The goal is to perform the data fusion, accept/reject decision, and removal all in real-time using FPGA technology.

Milestones

a) February 1, 2016: Determination of center of mass of each food item in image/line scan
b) September 1, 2016: Determine trajectory of food item for precise timing removal
c) February 1, 2017: Integrate hyperspectral data within food item edge boundaries
d) June 31, 2017: Use hyperspectral data within food item edges to classify food item as accept/reject
e) June 31, 2017: Time air jets to remove rejected food items
f) June 31, 2017: Final report emphasizing commercial products and potential

Progress toward objectives

A framework for the testbed system has been created for the hyperspectral waterfall sorting where a volumetric shaker feeder has been mounted on a steel cart (see Figure 2-1). Product such as lentils is put into the hopper and a vibrating 4 inch wide tray controls how fast the lentils fall into the 5 gallon bucket on the bottom shelf of the cart. The lentils fall in front of the airjet manifold where there will be 32 airjets that will be independently controlled to eject unwanted product such as bad lentils. The 32 airjet valves have been purchased that can open/close in ~ 1 msec.

Figure 2-1. Shaker feeder on steel cart

The airjet manifold (Figure 2-2) has been design with 32 air jets (line of holes in center) and 32 air valves (rectangular blocks) and is currently being constructed.

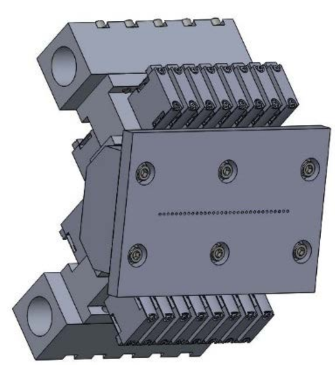

Figure 2-2. Airjet manifold for sorting system.

A poster on this work was presented at the 2016 conference of the MSU Optical Technology Center by undergraduate and graduate students Connor Dack, Sam Kysar, and Monica Whitaker (Figure 2.3).

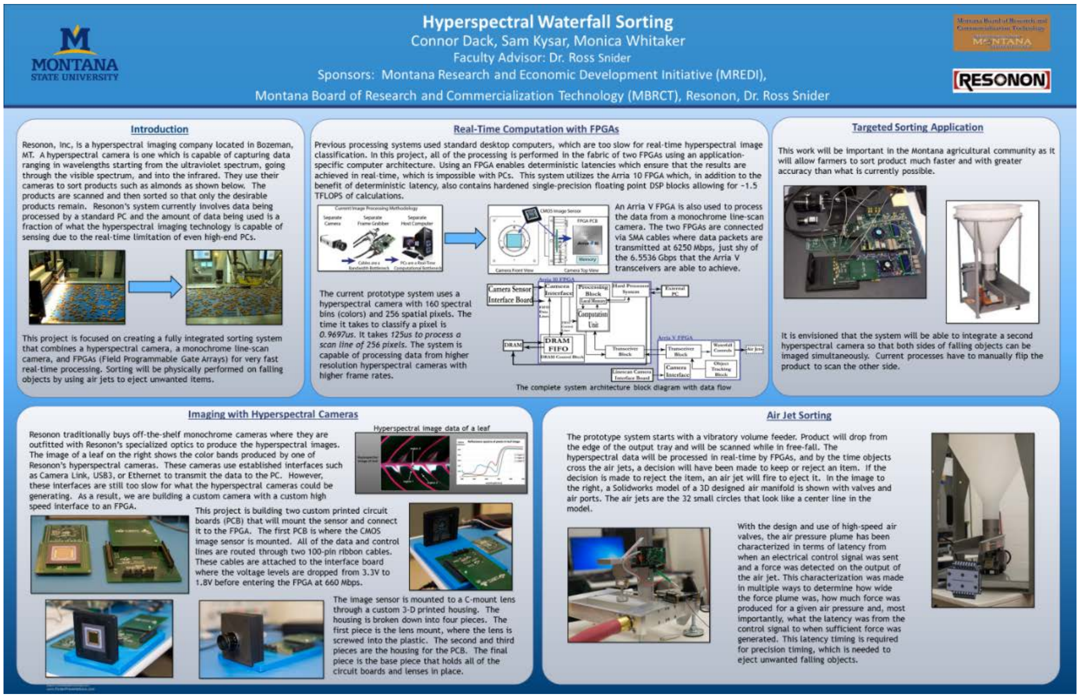

Figure 2-3. Poster presented by MSU graduate and undergraduate students at the 2016 annual OpTeC conference.

The high-speed serial links (6 Gbps) are now working between the Arria V FPGA board and the Arria 10 FPGA board (silver coax cables in Figure 2.4).

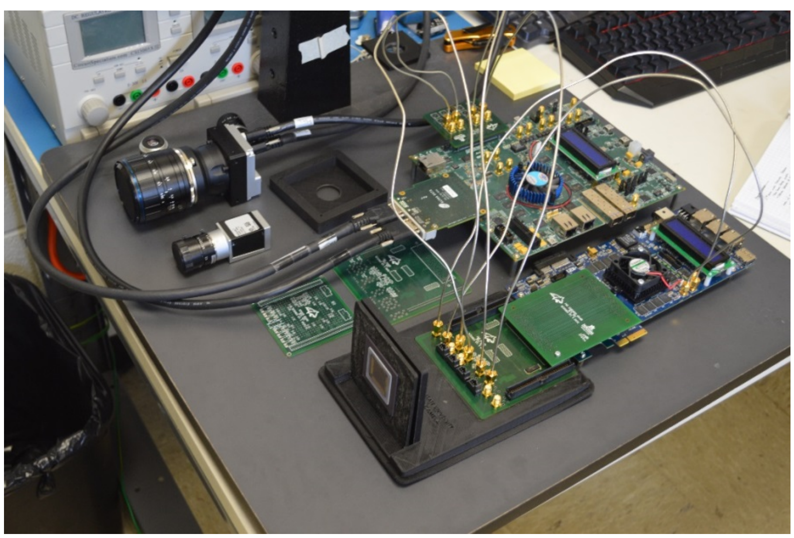
Figure 2-4. High-speed serial links between Arria V FPGA board and Arria 10 FPGA board.

Expenditures to date (41W411)

Personnel to date $27,714.70, Benefits $874.36, Operations $64,821.52, Capital equipment $4845.00; Total Expenditures **$98,245.58**.

Subproject 3: Remote Sensing Algorithms for Precision Agriculture (Rick Lawrence with Resonon, Inc.)
Develop and apply a methodology using hyperspectral imagery for determining optimal narrow spectral band combinations for identifying targeted invasive weeds in specific crops.

Milestones

a) July 31, 2016: Collect invasive weed field data
b) August 31, 2016: Collect hyperspectral image data
c) October 31, 2016: Complete image preprocessing
d) January 31, 2017: Complete analysis of spectral band optimization and weed species mapping
e) June 30, 2017: Final report, including applications for commercial site-specific agriculture

Progress toward Objectives

- Working with data to determine limits
- Presented at MREDI Legislative tour
- Created method for selecting of sample pixels
- “CompareMethods” R program adapted to research
- Band selection protocol run and output bands used in “CompareMethods” (Figure 3-1).

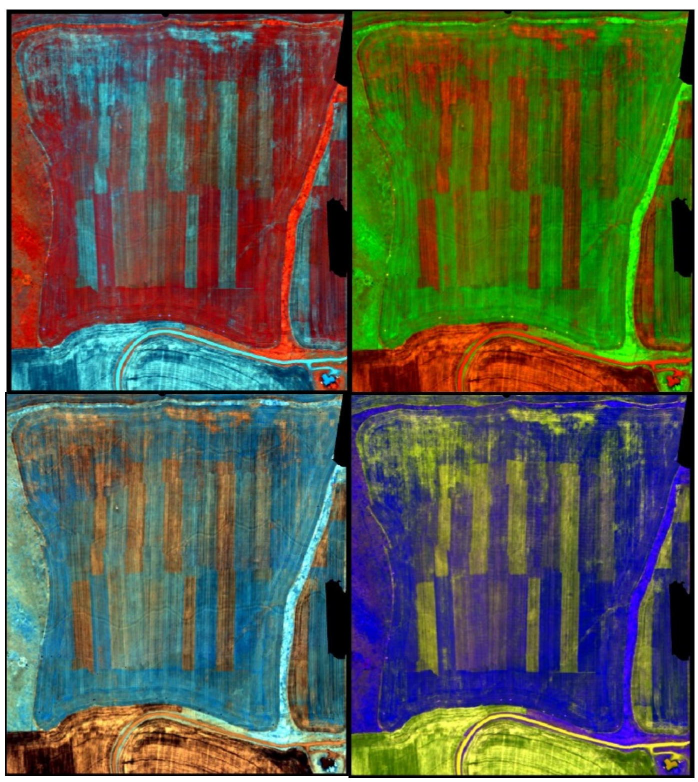

Figure 3-1: 3 Initial band combinations and false color IR. top left False IR 50/20/10, top right 18/61, bottom left 46/48/52, bottom right 20/39/58

Pixels in Pika II hyperspectral data of infested and un-infested locations were selected using field data. Four pixels per location were selected by converting GPS point data to polygons. Polygons were then used to select pixels and entered into ERDAS Imagine to output potential bands. Some potential band combinations from initial combinations can be seen in Figure 3-1. “CompareMethods” program in RStudio was adapted to research and a few initial band combinations run. This program runs 11 classification methods and outputs the accuracy and other important statistics (Figure 3-2).

```
[1] "C5.0"
Confusion Matrix and Statistics

          Reference
Prediction clean weed
     clean     7    3
     weed      7   10

               Accuracy : 0.6296
                 95% CI : (0.4237, 0.806)
    No Information Rate : 0.5185
    P-Value [Acc > NIR] : 0.1679

                  Kappa : 0.2663
 Mcnemar's Test P-Value : 0.3428

            Sensitivity : 0.5000
            Specificity : 0.7692
         Pos Pred Value : 0.7000
         Neg Pred Value : 0.5882
             Prevalence : 0.5185
         Detection Rate : 0.2593
   Detection Prevalence : 0.3704
      Balanced Accuracy : 0.6346

       'Positive' Class : clean
```

Figure 3-2 Output for one Classification method from ComparMethods

<u>Expenditures to date</u> (Grant 41W417) Personnel $30,179.55, Benefits $2,490.99, Operations $11,459.39; total Expenditures **$44,129.93**

Subproject 4: Machine Vision Algorithms for Precision Agriculture (Neda Nategh with Resonon and NWB Sensors, Inc.) Develop machine vision algorithms for weed detection and food sorting using spectral imaging data.

<u>Milestones</u>

a. Sep. 30, 2016 Initial testing of machine vision algorithms complete.
b. May 31, 2017 Final testing and development complete.
c. June 30, 2017 Final report completed.

<u>Progress toward objectives</u>

- Students were advised on the analysis of hyperspectral image data and statistical modeling
- Several new proposals were submitted based on a similar idea proposed in the MREDI Optics project.
    - “Google Faculty Research Award” – Google Inc. - $50,000.
    - “Sony Faculty Innovation Award” – Sony Electronics Corporation of USA - $100,000.
    - “Space debris identification and tracking system based on a real-time, bio-inspired motion processing algorithm” – NASA - $750,000.

<u>Expenditures to date</u> (Grant 41W413) Personnel $74,089.29, Benefits $5,673.17, Operations $10,802.90, total Expenditures **$90,565.36.**

Subproject 5: Microcavity sensors for hyperspectral imaging (Zeb Barber with Advanced Microcavity Sensors LLC). Advance MSU/Advanced Microcavity Sensors LLC (AMS) technology on microcavity hyperspectral imaging sensors toward commercial applications in agriculture and engineering tests to determine feasibility of mounting sensor technology on UAV; secondary objective solving MT problems in agriculture and biomedical (skin cancer). The primary objective focused on MREDI goal #2: creating private sector jobs.

Milestones

a) June 1, 2016: Investigate non-circular symmetric micro-cavity mirrors for transverse mode manipulation
b) September 1, 2016: Evaluate Microcavity Hyperspectral Imaging prototype system for early crop disease/weed detection
c) December 30, 2016: Determine engineering specifications for use of Hyperspectral Sensor on UAV
d) June 30, 2017: Submit final report specifying technical accomplishments and outlining commercial potential.

Nontechnical highlights

- Caleb Stoltzfus presented a poster entitled "Liquid Crystal Arrayed Microcavities (LCAM)" at the annual OpTec meeting on October 4th, 2016 in Bozeman, MT.
- MSU Spectrum Lab's AF STTR Phase II collaboration and project with Spectral Molecular Imaging, Inc. of Beverly Hills, CA and Advanced Microcavity Sensors was kicked-off with a meeting of all parties and the Air Force program monitors in Bozeman, MT.
- Dr. Daniel Farkas, collaborator from Spectral Molecular Imaging, gave an OpTec colloquium on Sept. 29th 2016.

Technical Progress toward Objectives

a) MSU Spectrum Lab continued work on characterizing the crater and cavity profiles constructed by Advanced Microcavity Sensors. To characterize the spectral properties of our novel LCAM optical filters we built a comprehensive testbed, shown in Fig. 5-1. This testbed allowed us to measure the free spectral range (FSR), the tuning range ($\Delta\lambda$), and the spectral resolution (FWHM) of LCAM filters with and without craters ablated onto the mirror surface.

The spectral response of LCAM filters was measured by recording the spectrum of the transmitted light for different voltages across the liquid crystal. A spectrum was recorded every 0.01 volts for voltages ranging from 0 to 10 volts. The spectral response of two LCAMs with and without craters are shown in Fig. 5-2. In these figures the voltage across the liquid crystal is on the y axis and the transmission wavelength is on the x axis. The plots are color coded such that brighter colors correspond to more light transmitted through the LCAM, with red being the most transmitted light and dark blue being no transmitted light. The liquid crystal does not respond to voltages under 1 volt. Above one volt the liquid crystal molecules begin to rotate resulting in a change in the index of refraction and a change in the peak wavelength of the spectral transmission window. As we expected, the LCAM with craters has better spectral resolution than the LCAM with no craters.

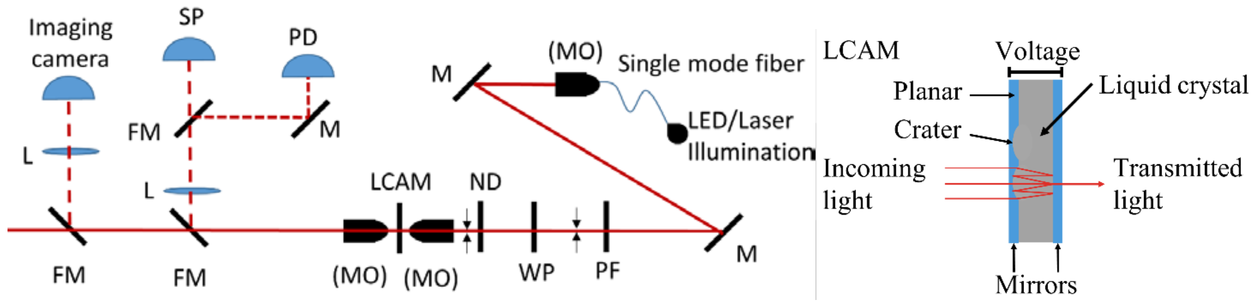

Figure 5-1. Left| Schematic of the LCAM characterization testbed. M-Mirror, MO-Microscope objective, FM-Flipper mirror, WP-Wave plate, ND- Neutral density filter, PF-Polarizing film, SP-Spectrometer, PD-Detector, L-Lens. Right| Schematic of a LCAM optical filter.

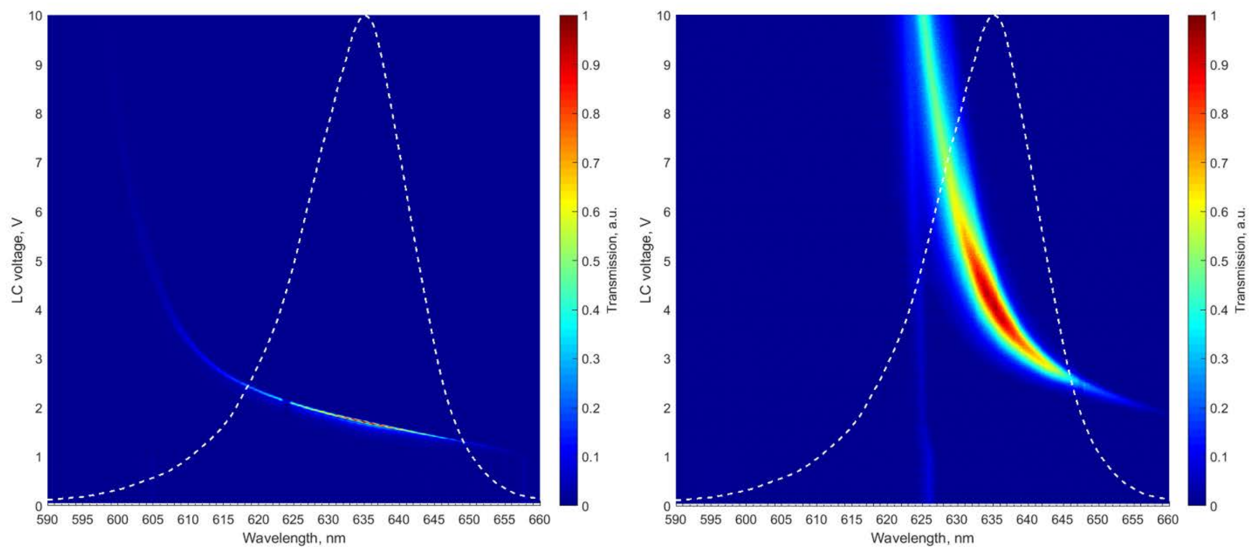

Figure 5-2. Left| Spectral response of an LCAM with craters ablated into one of the mirror surfaces. FSR= 58.5 nm, $\Delta\lambda$=53 nm, FWHM < 1 nm | Spectral response of an LCAM with no craters. FSR=80nm, dl=55nm, FWHM > 3.6nm. The white dotted lines show the spectra of the unfiltered LED light that is incident on the LCAM.

b) As discussed in the last quarterly report, the Spectrum Lab came to the conclusion that most agricultural applications are ill-suited to the high spectral resolution provided by the LCAM. For this reason, we have re-evaluated application areas more suited to the LCAM. Two areas stand out: passive optical sensing of atmospheric gases and the microcavity-based dye laser application that will be funded by the MBRCT.

During the last quarter, we reported that a new proposal on multi-wavelength independently tunable microlasers was submitted to MBRCT. This proposal has been selected for funding by MBRCT and the work will be carried out at Spectrum Lab, MSU and AMS, a local company that licenses this technology. This work is scheduled to start during this quarter. This laser array proposal leverages the LCAM technology, pioneered by AMS and Spectrum Lab, and is currently supported by the MREDI project. Key value propositions for the laser array concept are – (1) Ultra-low lasing threshold reduces power requirements: 2) Physical size and portability: and 3) Scalability of the array architecture.

This new product will be an excellent complementary product line to the hyperspectral imaging sensor currently under development at AMS. It is anticipated that the laser array will be ideally suited for Raman imaging since it matches well with the LCAM based hyperspectral imaging sensor. This is not easy to achieve in current spectral imaging systems due to lack of a practical source that allows efficient illumination.

This project will focus on demonstrating a few channels of lasing, independent wavelength tuning and low power operation, while ensuring that the package has minimal opto-mechanical footprint. Although the initial applications for this project are likely to biomedical and spectroscopic, it is expected the new technology would provide a good fit for many applications being pursued by local photonics companies and will add significant value the Montana optics industry.

c) We have not made significant progress on this objective. However, we are continuing to determine that the liquid crystal tuning approach is superior to piezo-electric tuning for stability. During this quarter collaborating with AMS we worked on constructing more compact versions of the microcavity optical system. The system shown in Figure 5-3 couples fiber delivered light to a single microcavity using a stable and compact cage mount system. Further compaction can be achieved using more permanent mounting systems including the use of microlenses.

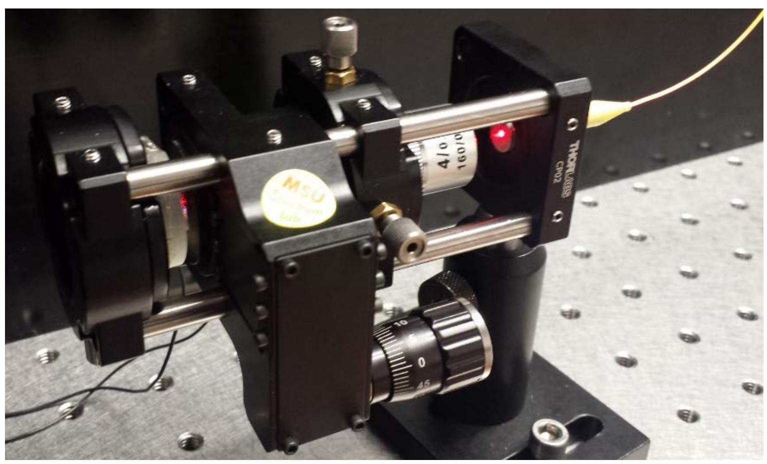

Figure 5-3. Compact and stable LCAM characterization system.

<u>Expenditures to date</u> (Grant 41W418) Personnel $32,980.03, Benefits $11,639.96, Operation $1,765.97, total Expenditures **$46,385.96** Expenditures greatly increased due to a gap in funding from the AF STTR and the MBRCT.

Subproject 6: Hyperspectral imaging for monitoring cell growth (Ed Dratz, dratz@chemistry.montana.edu with Resonon, Inc.). Design a hyperspectral imaging system for monitoring the metabolic state of live cells in culture. Applications to stem cells for understanding disease mechanisms in individuals, drug testing in cells from individuals, potentially optimize personal nutrition, and solve Montanan's health problems.

Milestones

a) February 1, 2016: Complete design and testing of proof-of-principle prototype hyperspectral imager with improved cost/benefit, prototype interface for cell hyperspectral analysis, and development of stem cell labeling.
b) May 1, 2016: Integrate the prototype systems for advanced analysis of stem cell metabolism with hardware and software control. Test for evaluation of optimization of selected nutrients.
c) October 1, 2016: Refine and improve software and operating conditions of real time hardware and software for variations of metabolic state for culture optimization.
d) February 1, 2017: Enhance user interface to control system and software to control and optimize nutrient composition; evaluate possible changes in microscope system for improved performance.
e) June 30, 2017: Proof of principle for feedback control of nutrient optimization with nutrient dosing control system. Investigate biochemical individuality in pilot experiment.
f) June 30, 2017: Submit grant proposals to leverage additional support. Final report to MUS that summarizes accomplishments and commercial potential.

Activities to date

There are six components that need to be integrated to complete this project. The hyperspectral microscope system, the high-speed and high-accuracy sample stage, the microfluidic nutrient dosing and cell growth chamber system, the control and analysis software, and the integration and testing of the fluorescent sensors of the metabolic state of the human adult stem cells. Progress has been made on all of these components.

The inverted epifluorescence microscope optical system has been designed, optical vendors contacted for providing optical modules, the optical system has been configured, and all the microscope components have been selected, as reported in the Q4 report. We were able to find a single vendor, ASI, to provide an integrated, high-performance inverted microscope solution, where all the components are sure to fit together with appropriate focal lengths and where the specialized hyperspectral components can be fitted. Furthermore, this US vendor, as the only US manufacturer of integrated microscope systems and will provide the best possible price on the complete optical systems. This excellent price for the optical components will facilitate the commercialization of the complete hyperspectral microscope with the integrated microfluidic cell culture system and complete, powerful computer control and software system that is under development. We have an upright, laser-excited fluorescence microscope test bed at Resonon for testing the hyperspectral microscope system. We expect that the hyperspectral components in hand can be integrated with the modular inverted microscope, as soon as the inverted microscope parts arrive. The inverted microscope system is essential for viewing live cells and monitoring their metabolic state, which is at the center of this project.

Progress has been made on software to drive the computer-controlled XY sample stage, which has to scan in small, very high-resolution steps for maximum hyperspectral resolution (22 nm in this case), along with rapid movement speed (7mm/sec in this case), so we can rapidly revisit cells in the field for repeated spectral measurements after modifying the nutritional state.

The ASI Company, in Portland, has also expressed interest in teaming with us to refine the development of our planned commercial product. The microscope will do an initial rapid scan of the image field, the software will locate cells, and the cells will then be scanned at high resolution repeatedly during the course of the experiments. Thus, the stage has to be able to scan rapidly between cells and then switch to much slower, small step sizes for high- resolution imaging. The software control for the XY stage and Z automatic focusing with programmable nose piece for changing objectives for different magnifications is in prototype and will be tested as soon as the stage arrives. The upright epifluorescence microscope test system from the Dratz Lab that was moved to the new Resonon facility is being used for initial testing of the excitation laser system for hyperspectral imaging.

The Onix CellAsic microfluidic cell culture control and observation system has been upgraded with a new model, just released, and that new model has been supplied to us gratis (about $20,000 value), since the vendor, Millipore is interested in supporting our project. The new Version 2 of the Onix CellAsic microfluidic cell culture control system has been installed on the refurbished laser- confocal (The Zeiss LSM 510 meta), with the latest image analysis software, that is important for providing benchmarks for the new hyperspectral system. This microscope is a high-performance confocal, with the latest image analysis software, that is important for providing benchmarks for the new hyperspectral system. Prof. Snider’s team is working on the software to integrate the Onix CellAsic microfluidic culture control with the hyperspectral data acquisition and processing. Prof. Snider’s team has set up their computer control system in our microscope room for testing of the control software for the CellAsci cell culture control system and the high performance, computer controlled microscope stage. We desire an integrated software package that can analyze the hyperspectral data, control the microscope stage and microscope magnification, and the nutrient stimulus and all the software components are progressing well.

A great deal of progress has been made in the Dratz lab on introducing optogenetic probes of the oxidation/reduction state into human adult stem cells in culture. The probes have been transferred to efficient carrier vectors that are providing improved, more facile optical probe introduction. We have also introduced the optogenetic probes in to Murine smooth muscle cells to demonstrate the wide applicability of our systems for metabolic monitoring of live cells. There is a great deal of local experience with these smooth muscle cells and monitoring the control of the metabolic state if these cell lines. A graduate student in the Dratz lab is devoting full effort to working with the optogenetic probes, assisted by a research undergraduate, two postdoctoral in the Reijo Pera lab, and Robert Usselman, a Research Assistant Professor in the Singel lab, all in the MSU Chemistry and Biochemistry Department. An undergraduate Electrical and Computer Engineering (ECE) design team in the Snider lab in ECE is continuing to design the microscope stage controller system and the controller for the cell culture environmental control system. A graduate student in the Snider lab is devoting full effort to the high-speed hyperspectral imaging analysis software. The personnel include two graduate students devoting full effort to the project and two advanced undergraduates on an ECE Design team.

Expenditures to date (Grant 41W414) Personnel $44,254.86, Benefits $8,975.81, Operations $25,294.73, Capital Equipment $29,261.20; total Expenditures **$107,788.60**

Subproject 7: Translational research to commercialize micro-mirror technology (Arrasmith at Revibro Optics). Translate MSU-developed deformable mirror technology to a commercially sustainable product.

Milestones

a) June 30, 2016: Refine production to achieve a repeatable fabrication process. This milestone will involve a redesign of fabrication masks, purchase of new wafer bonding equipment, and refinement of wafer bonding process
b) Obtain funding from another source. Revibro will pursue funding through commercial sales and commercial R&D efforts (June 2016), and through SBIR/STTR or similar government funding (June 2017)
c) Create 2 full time Montana jobs: One job will be created immediately to sustain the founder of Revibro – August 2015; Technical and/or sales and marketing hire – December 2015

Progress toward objectives

- Revibro received its first 2 commercial purchase orders!
- Hired our first full time employee
- Redesigned fabrication masks and began fabrication to improve repeatable production of mirrors

Q5 has been an exciting quarter for Revibro Optics. Directly related to Milestone b, we received our first two purchase orders in August, one for our "standard" mirror prototypes and one for custom mirror development. We have been working hard to fabricate new mirrors and fulfill these orders by the end of the year. This marks the first commercial revenue that Revibro Optics has received, and we are hopeful that we will continue to receive interest as these early adopters spread the word about our technology. We are also continuing to pursue SBIR funding to sustain the company for the next few years during the growth of commercial revenue.

Revibro Optics also hired a full-time engineer recently. This hire took place mid-October. This engineer is currently working full time to support the fabrication efforts, and will extremely valuable to support future design and engineering efforts. This hire accomplishes Milestone C by creating 2 full time Montana Jobs.

To accomplish Milestone A, Revibro did a thorough redesign of our fabrication masks for our standard 4mm mirrors in July. The masks were received in August, and we have been working for the months of September and October to use these masks to fabricate new mirrors. The goal of this milestone is to improve our fabrication process, both through new mask design and new fabrication techniques, to achieve higher yield of our mirrors. By the end of Q6 we will be able to evaluate the effect of the new mask design on device yield, and will begin to design an improved wafer bonder. We are also working with MSU to find a suitable commercial wafer bonder that would benefit both Revibro Optics and other companies and research groups on campus.

Total Expenditures: (Grant 41W410 Sub-Award) Personnel & Benefits $93,652.99, Total Expenditures **$93,652.99**

Subproject 8: Active waveguides and integrated optical circuits (Rufus Cone, cone@physics.montana.edu, collaborating with Babbitt, Nakagawa, Barber, Himmer, Avci, and Thiel with S2 Corp., AdvR, FLIR/Scientific Materials, and Montana Instruments). Integrate Montana products, expertise, and capabilities to improve marketability, performance, and enable additional products: Build interdisciplinary connections among MUS and Montana optics industries to integrate (a) optical crystals by FLIR/Scientific Materials Corp. (SMC); (b) waveguide photonic components of AdvR, Inc.; (c) Montana Instruments (MI) cryogenic systems; and (d) S2 Corp. (S2C) signal processing devices.

Milestones:

a) Fall 2015: Fabrication of rare earth doped optical waveguide suitable for optical signal processing applications
b) Summer 2016: Integration of an optical waveguide into a cryostat
c) Spring 2017: Demonstration of SSH processing in a cryogenic waveguide
d) June 2017: Final report summarizing technical results and emphasizing commercial potential

Activities to date

During this fifth reporting period, significant progress continued on all project activities. A wide range of coordinated research and development activities are progressing rapidly at this stage of our effort, most of which are in close daily collaboration with our Montana industrial partners. A primary focus of this quarter's efforts was the development of a range of new and enhanced techniques to characterize optical waveguide properties. In particular, several new methods that leverage the unique scientific and technical expertise of existing MSU research programs were developed, potentially with broader commercial applications beyond the current MREDI goals. These methods exploit coherent laser sensing as well as high-resolution spectroscopic capabilities at MSU. In addition to characterizing optical waveguide fabrication and device performance, coordinated work on all other aspects of the project continue, including cryogenic integration, material processing, and theoretical modeling.

In addition to those selected highlights from this quarter, additional outcomes are outlined below.

Progress on Technical/Educational Objectives:

New Methods for Nondestructive Characterization of Optical Waveguides

Traditional methods for determining waveguide propagation losses include what is termed the Cut-Back Method. The cut-back method is a way to separate the propagation loss through the waveguide from the coupling losses that occur at the input and output. In this method, the propagation loss (dB/cm) is estimated by changing the length of the waveguide and observing the change in loss. However, for accurate measurements, it is necessary to keep the coupling losses consistent across all loss measurements. This is relatively straightforward for optical fibers, but can be tricky for other types of waveguides—particularly those that are difficult to cleave, or require polishing or some other post-processing to acquire a clean facet.

Our ultra-high-resolution FMCW LADAR method of determining waveguide propagation loss is independent of input and output coupling losses. It relies on the backscatter signal from the back facet of the waveguide. This method should enable AdvR Inc. and other companies making optical waveguides and other micro-optic devices, such as splitters, interferometers, polarizers, switches, etc. to determine propagation losses without the extra cleaving process of traditional methods. This is a very significant improvement and ties directly to our goal of improving competitiveness of Montana companies.

The optical waveguides fabricated last quarter in MSU's MMF in cooperation with AdvR are now being tested using the nondestructive method developed using this MREDI grant support. A microscope image of a portion of a waveguide chip is shown in Figure 8-1. This method uses a frequency chirped-laser, a reference fiber interferometer, and signal processing algorithms. The test apparatus is illustrated in Figure 8-2, and a photo of the free space test path is shown in Figure 8-3. Here, we can measure the back scattering in a waveguide to determine waveguide propagation losses without destroying the waveguide as in the typical cut-back method. The photo in Figure 8-4 shows the laser correctly coupled into one of the optical waveguides. The frequency-sweep of the laser was not perfectly linear, so we used the reference interferometer signal to linearize the sampling in post processing. The balanced detectors used to capture the output optical signals were designed and fabricated at MSU Spectrum Lab. The captured signals are stored on the computer for post processing.

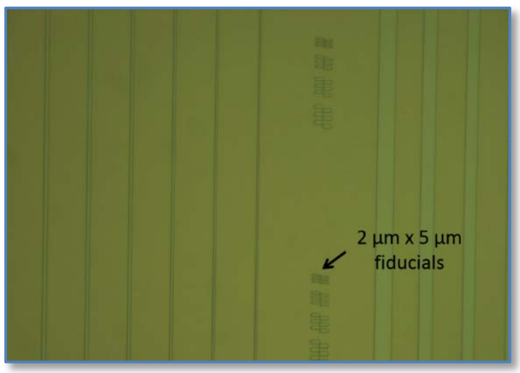

Figure 8-3. Microscope image of optical waveguides. The 2 µm fiducials are used to visually determine the quality of smallest fabricated waveguide diameter.

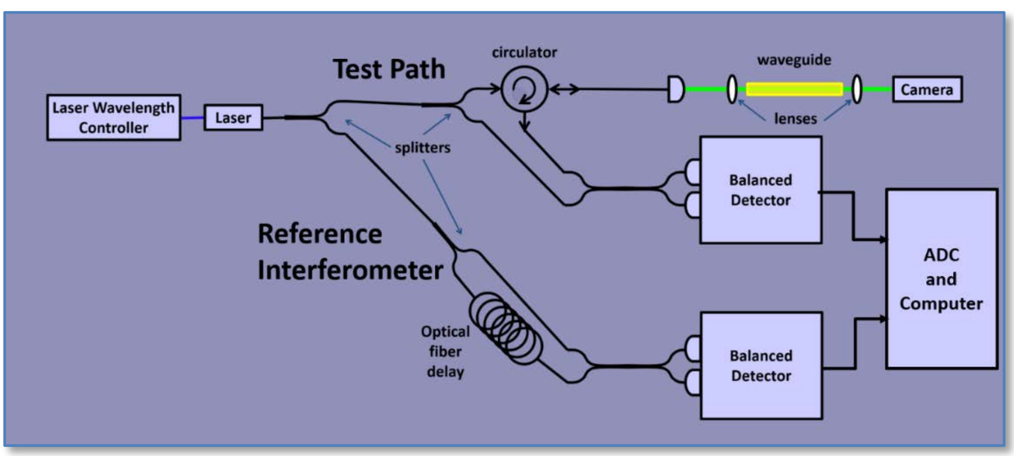

Figure 8-4. Test Setup for nondestructive optical waveguide characterization. An ultra-high resolution FMCW ladar signal is split between the optical waveguide path and a reference interferometer path. The interferometer signal is used in post processing to remove any nonlinearities of the laser chirp modulation. This method of determining waveguide propagation loss is independent of input and output coupling losses.

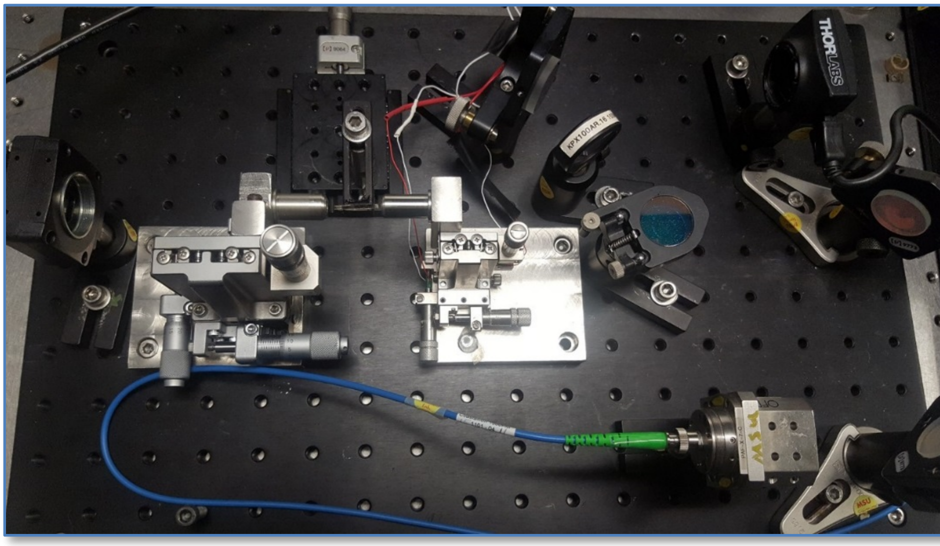

Figure 8-5. Photo of test path free-space section. The waveguide chip is positioned between two xyz-stages using an x-stage. A camera is used to image the coupled optical mode.

Figure 8-6. A guided optical mode captured on camera.

The plot in Figure 8-5 shows post-processed signals when the frequency-swept laser is coupled above the waveguide chip (green), below the waveguide yet in the substrate (red), and into a waveguide (blue). The guide coupled mode is verified with a camera image as shown in Figure 8-4. The first peak coinciding in the red and blue traces correlates to the chip's front facet. The next two peaks in the blue correspond to first and second reflections off of the waveguide back facet. The measured propagation loss of the waveguide is half the difference of the two peak heights divided by the chip length. Results of our new method compare well with the cut-back method now used at AdvR Inc. for optical waveguide propagation losses.

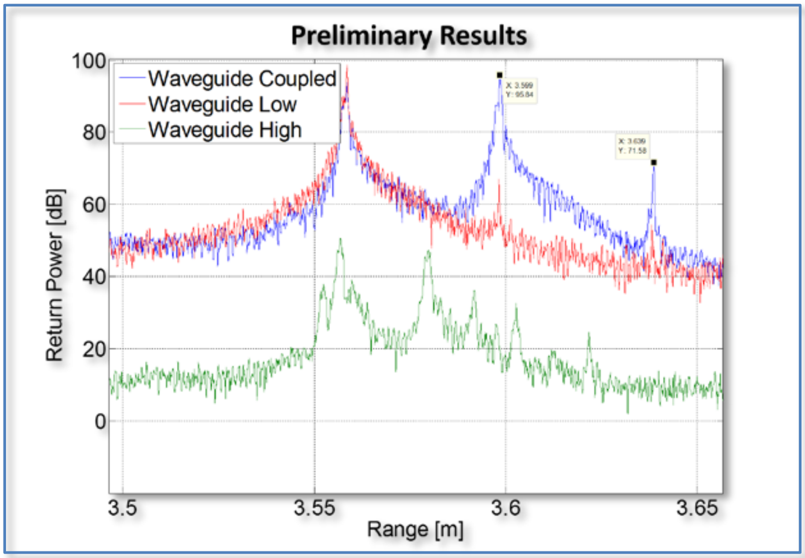

Figure 8-7. Post processed signals from the balanced detectors. The blue signal is a correctly coupled into a waveguide result. The green and red signals are results of the chirp laser signal being above the waveguide and below the waveguide yet in the substrate, respectively. The coinciding peak of the coupled and low signals refers to the front facet of the waveguide chip. The next two peaks in the coupled signal correlate to the first and second reflections off of the waveguide back facet.

To aid in alignment and guide coupling a second camera, lens, and beam splitter for visible light were added to the free space test path. The input coupling lens and the new lens create a telescope to image the front facet of the guide chip. Details are shown in Figure 8-6, and a camera image of the front facet is shown in Figure 8-7. The beams splitter acts like a mirror to the ~1550 nm wavelength laser light and allows some of the light from the white light source to pass to the added camera. With this setup the guided laser beam and the front facet may be viewed simultaneously with images like those shown in Figure 8-4 and Figure 8-7.

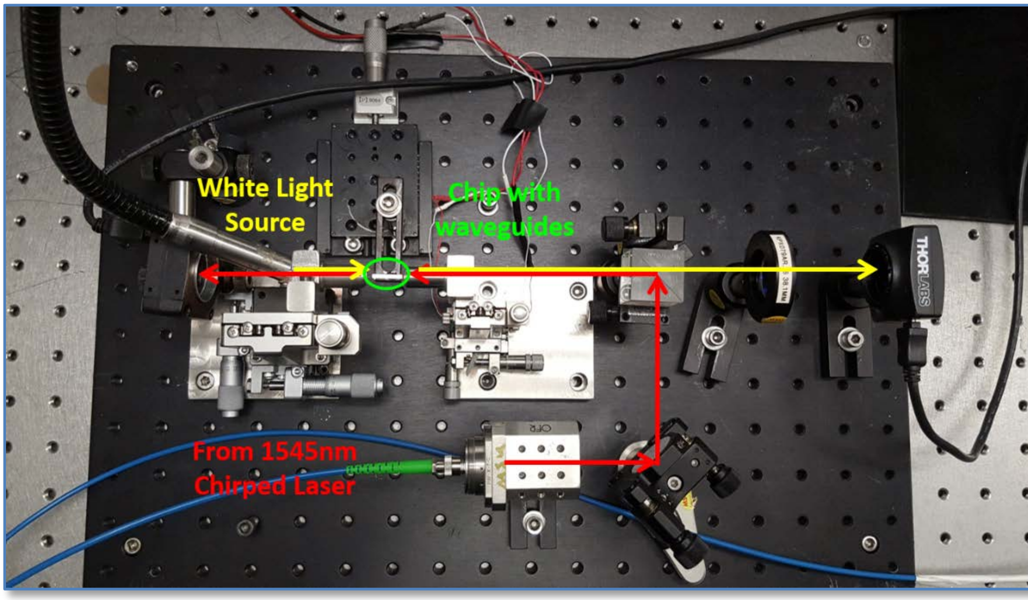

Figure 8-8. Added components for assisting in alignment and coupling light into waveguides include a white light source, a beam splitter designed for visible light, a lens, and a visible light camera. The beam splitter acts like a mirror to the 1545 nm laser light. The input coupling lens and the new lens form a telescope. The white light source and the camera provide visualization of the waveguide chip front facet.

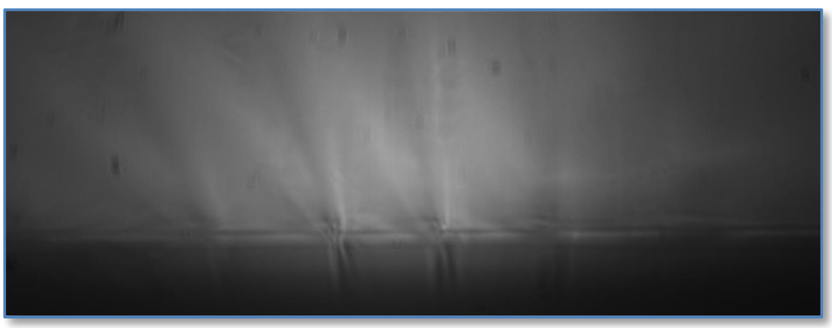

Figure 8-9. Camera image of the waveguide chip top front facet showing a few waveguides.

Study of Optical Waveguides at Cryogenic Temperatures

Basic characterization of the polarization of modes of a proton exchanged waveguide in a Montana Instruments Cryostation has been carried out at 3 Kelvin with free-space coupling. A new adaptor plate was fabricated to hold the waveguide and output coupler lens and attached to the sample mount in the Cryostation, demonstrating the ease of reconfiguring the system to new applications. The waveguide modes were found to be spatially distorted from room temperature modes due to strains in the host material, but the low-temperature modes still supported the room-temperature polarization in the guides. These measurements inform us that thermal strain in the crystal bulk is presently a limiting factor in minimizing loss in the guide at low temperature. By increasing the amount of light supported by the waveguide at low temperature, more advanced measurements of the basic properties of the guides can be made much more easily and accurately.

Figure 8-10. Example of optical fiber coupling of AdvR Inc waveguide within a Montana Instruments Cryostation.

In addition to the free-space optical coupling, work has also progressed on integrated optical fiber coupling of waveguide components into the cryogenic environment. Initial studies have employed compression vacuum feedthroughs provided by Montana Instruments to transition the glass optical fibers into the cryostat, with free-space optical output from the fiber coupled waveguide, as shown in Figure 8-8.

Characterization of Waveguide Properties

Basic properties of fabricated optical waveguides, such as the numerical aperture and the effective refractive index of waveguides, are generally difficult to measure and corroborate with other evidence. Experimental techniques are being developed to measure these characteristics accurately and reliably. The numerical aperture has been measured by determining the angle at which the light diverges from the waveguide. This measurement not only assists in improving the coupling efficiency into the waveguide by matching the numerical apertures of the input coupler and the guide, but also provides information on the shape of the mode in the guide. The refractive index of materials has also been measured with a coherent laser technique using an optical frequency sweep in a Michelson interferometer apparatus constructed during this quarter. By honing the interferometric technique for increased accuracy and then applying it to a waveguide, the effective refractive index for different optical polarization states can be directly measured. This new method offers an essential capability by which the refractive index and guiding properties of modified waveguides can be consistently measured.

Numerical Simulations of Rare-earth-ion Resonance Lineshapes

Monte Carlo numerical simulations are being developed to facilitate theoretical and experimental descriptions of interactions of ion-ion interactions in rare-earth-activated materials. These simulations provide a theoretical tool to identify possible microscopic interactions between atoms in a material. This capability will allow material performance in optical signal processing applications to be predicted and will provide key information about practical device scalability requirements and limitations for each potential optical material system.

Development of an Improved Thin Film Vacuum Deposition System

The simple thermal evaporation vacuum deposition chamber has been rebuilt with improvements to many of its components. New electrical feedthroughs and electrodes, chamber body, seals, heaters, and a water-cooled precision quartz crystal oscillator have been added to improve reliability and consistency, increase ease of use, and lower the time needed to perform a deposition. This extends our capabilities for waveguide fabrication and material modification. The new deposition chamber has been used deposit layers of Erbium and Thulium onto $LiNbO_3$.

Investigation of Deuterium-Exchanged Optical Waveguides

Many traditional waveguides use proton exchange to produce the guiding channel. Continuing with our efforts to produce novel rare-earth-activated optical waveguides with properties optimized for signal processing applications, a new chemical process for fabrication is in progress in the lab; this method replaces the standard proton exchange process for $LiNbO_3$ with exchange of the heavier deuterium isotope of hydrogen. The increased mass of the deuterium ions is expected to modify the microscopic vibrational dynamics of the waveguide, potentially improving the resonant optical properties of rare-earth-ions that are incorporated into the waveguide.

Development of Sub-micron Periodically-poled Nano-photonic Devices

There has been important progress towards the fabrication of sub-micron periodically poled ferroelectrics. Several microfabrication procedures for the creation of poled electrodes were improved. The first fully fabricated wafer of electrodes was completed, and the wafer was diced into individual electrodes by Bozeman company AdvR Inc. With AdvR's collaboration, preliminary poling tests were conducted on lithium niobate waveguide crystals. Analysis of the poled crystal showed examples of successful periodic poling, a promising preliminary result.

In preparation for future application of our periodically poled crystals, several modeling efforts were undertaken. A program was developed to calculate the necessary period of poled domains to achieve quasi-phase matching (QPM) for various nonlinear frequency conversion processes, which included variation of signal and pump wavelengths and propagation directions. A second program was created that models the coupled differential equations for counter-propagating three wave mixing. Together, these programs are useful for determining necessary grating periods and expected conversion efficiencies for the various nonlinear processes. Lastly, a program was created that calculates the bandwidth acceptance of the various frequency conversion processes for specific computed optimal grating periods. Large bandwidths were found in the case of certain three wave mixing processes that could be of significant importance to potential applications.

We have been analyzing the benefits afforded to various applications through use of sub-micron-domain periodically poled waveguides. One application is differential absorption LIDAR (DIAL). Dr. Kevin Repasky (MSU, Electrical Engineering) is developing a high sensitivity DIAL measurement system to measure atmospheric composition (such as methane density vs height). The system could benefit from a device that could convert extremely low-power infrared DIAL return signals (down to the single photon level) into the visible spectrum, where higher sensitivity optical detectors are available. Counter-propagating sum-frequency generation with sub-micron QPM periodically poled crystals has the potential to achieve the performance needed.

This work has led to the development of a proposal for further funding of sub-micron poling research. The proposal will be submitted at the end of October to the National Science Foundation with Wataru Nakagawa in MSU Electrical Engineering as the principal investigator.

Testing Vibrationally Induced Coherence Loss in Closed-cycle Cryostats

The results of the previous quarter were presented by graduate student Aislinn Daniels as a poster at the OpTeC Conference in early October. This quarter, we focused on improving the cryocycle triggering circuitry for the available Cryomech cryostation (the cryostation with the modified sample chamber and mount from S2 Corporation). The triggering circuit designed and built last quarter, which sensed, filtered, and squared the sound of the helium gas flow during the cyrocycle, resulted in significant timing jitter (on the order of 20 milliseconds rms), as well as major outliers (false triggers). To reduce this a new circuit was built which taps into the electrical signal transmitted from the cryostation compressor to the cold head. This signal is then filtered, converted into a binary signal, and divided to match the frequency of the cycle. This new electrical signal acts as the trigger to the system. The timing of this trigger is not synched with the start of the cryocycle, so its timing is compared to the previous audio triggering signal and the temporal shift is accounted for in the experimental design. Experiments to test the new circuitry are currently underway. The setup will then be used to complete the study of coherent loss during the cryocycle. The timing circuitry also is essential for the planned development of the passive microwave imaging system, which uses the cryogenically cooled spatial spectral material as a sensitive broadband correlator.

Development of Improved Laser Characterization Capabilities at New Wavelengths

Undergraduate Riley Nerem began construction of a series of low-cost Scanning Confocal Fabry-Perot Interferometers (SFPI) that allow the spectral structure of lasers to be measured at wavelengths that cannot be currently studied using standard commercial systems. The SFPI's will allow improved longitudinal mode characterization of lasers and, upon successful testing, will be replicated for a wide variety of wavelengths used in the lab. The improved measurement capabilities will be especially applicable to the new low-cost external cavity diode lasers being developed as part of our MREDI effort.

Study of the Effects of Chemical Processing on Optical Absorption Spectra

Studies were initiated to explore the effects of varying the oxygen content of the $LiNbO_3$ host crystal on the erbium absorption line at 1.5 micron telecommunications wavelength. The oxygen content of the crystal was modified by treatment at high temperatures in atmospheres with controlled oxygen content or in vacuum. For example, treating the $LiNbO_3$ in vacuum pulls oxygen out of the crystal changing the absorption spectra due to increased disorder, while also affecting other properties such as electrical conductivity and optical damage resistance. These measurements can also give insight into how oxygen stoichiometry can be used to change the optical properties of the material such as the UV absorption band and index of refraction and also how the oxygen stoichiometry affects the rare earth ion transitions. Initial studies have shown that even large variations in oxygen content do not significantly affect the static spectral properties of the rare-earth ion, suggesting that this may be a promising approach for modifying the bulk crystal properties without degrading the resonant optical properties. Additional studies are underway to explore the effects of the oxygen content of the dynamic properties of the resonant optical transitions.

Development of Fluorescence and Raman Microscopy Waveguide Characterization Techniques

As part of our MREDI effort, a Raman and Fluorescence imaging microscope was obtained and refurbished to working order to enable study of microscopic chemical and structural variations in waveguide structures. The overall system is now being upgraded with a new computer to control and analyze data. This microscope will greatly enhance the lab's capabilities to characterize crystals studied both by the lab and by other groups. Initially, the spectral image filters and cooled CCD camera detection system are employed to study concentration dependence of rare-earth ions in waveguide structures, with detailed study of crystal phase using Raman spectroscopy being employed in later stages of the study.

Progress on Economic Objectives:

- MSU-Spectrum Lab received a subcontract of $181,000 from S2 Corporation on a AF Phase II SBIR entitled "Instantaneous Wideband 10 GHz Time Difference of Arrival" to advance the S2 and supporting technology for wideband correlation of RF signals to determine the time difference of arrival at widely separated antennas.

- While working on this MREDI effort, undergraduate student Kyle Olson (junior in Physics), wrote and submitted a successful research proposal for the 2016-2017 academic year that was funded by the MSU Undergraduate Scholars Program. Kyle's project is directly related to our MREDI goals and builds on his work during summer 2016 on studying the effects of waveguide fabrication on the properties of rare-earth ions in crystals. This student project will focus on developing entirely new capabilities at MSU for using advanced fluorescence and Raman microscopy techniques traditionally employed in the biological and geological fields to study and characterize rare-earth-activated waveguide devices fabricated at MSU and at the Montana company AdvR Inc. We anticipate that this will provide new insights into both the fundamental chemical variations in the crystalline waveguides as well as into the consistency, limitations, and routes for improvement for waveguide production methods.

- A public outreach display, shown in Figure 8-9, was constructed to demonstrate MREDI-enabled integration and enhancement of the various technologies and products of Montana optics and photonics companies.

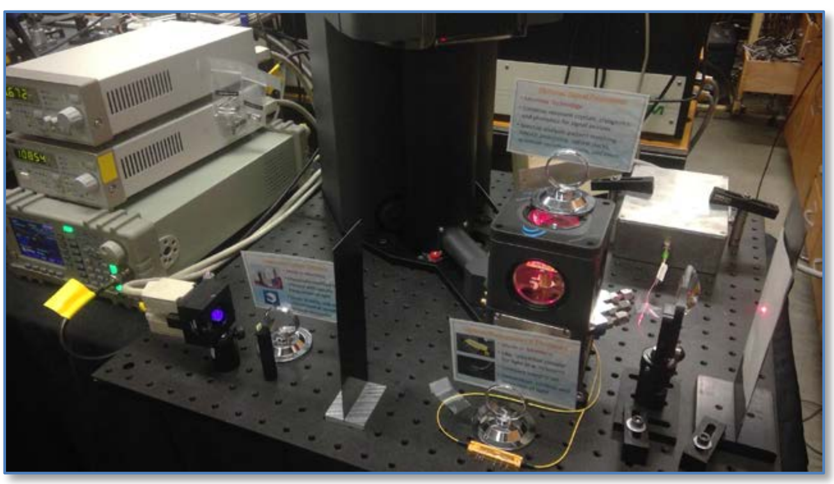

Figure 8-11. Demonstration system constructed to illustrate integration of Montana Instruments Cryostation with AdvR Inc waveguides, Scientific Materials Corp. crystals, and S2 Corp photonic signal processing.

- During Fall semester 2016, undergraduate and graduate students are enrolled for class credit in a weekly seminar series focused on MREDI and Spectrum Lab related research efforts.

- Dr. Gregory Reinemer from Highline College in Des Moines, WA visited the Cone-Thiel research group October 10-20, 2016 to work on development and testing of low-cost tunable external cavity diode laser systems. Dr. Reinemer worked in close collaboration with students Tino Woodburn and Kyle Olson to build a Littrow external cavity diode laser. The device was designed to be compact and easily reproducible using a gimbal mirror mount that was machined out to hold all the components of the laser. The first laser developed uses a red diode (650 nm), a 1200 lines/mm grating, and a mirror mounted at the same angle as the grating, enabling light to be easily coupled into a fiber, with the prototype shown in Figure 8-10. The laser diode current driver and assignment board for this laser was donated to Dr. Reinemer by Wavelength Electronics Inc, Bozeman. This interaction has initiated new conversations with other local optics companies, extending MSU-industry collaboration. The constructed laser will be used for educational purposes and provides as prototype for building new lasers at many different wavelengths of interest for our MREDI research efforts. In particular, a low-cost commercial blu-ray laser diode (405nm) has been incorporated into this external cavity laser design and is currently being characterized.

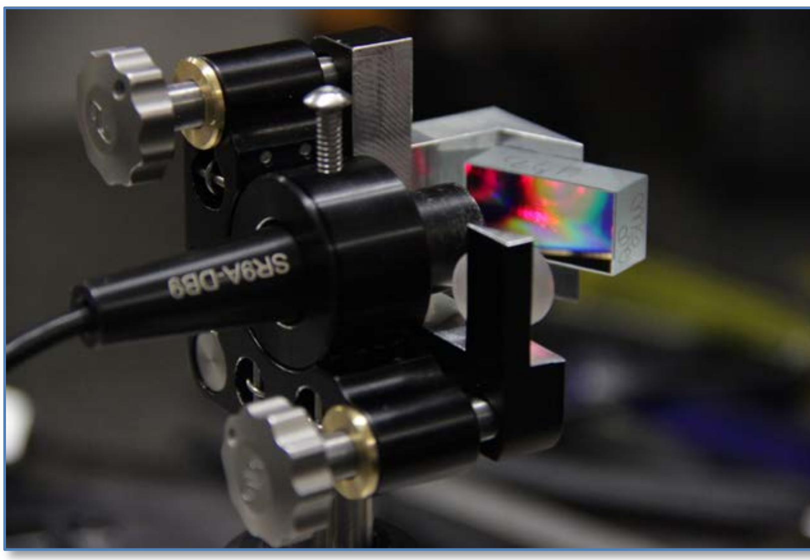

Figure 8-12. Simple and inexpensive tunable diode laser system constructed at MSU to enable new research and applications employing regions of the optical spectrum that have not been previously accessible for rare-earth-activated devices.

- In the previous quarter, we reported that S2 Corporation in consultation with Spectrum Lab contracted the growth of a Tm:$LiNbO_3$ signal processing crystal from United Crystals with S2 internal funds. Samples were provided to S2 Corporation, but upon inspection they were shown to have significant optical scattering and in one sample large refractive effects. However, surprisingly much of the large refractive effects and optical scattering of these samples seemed to disappear after the sample pieces rested for a few weeks. Further scattering analysis performed by Spectrum Lab showed several small defects in one sample. However, the defects were small enough to allow a clear path for further laser testing of the material.

- In collaboration with MSU Spectrum Lab, S2 Corporation has contracted the growth of a new Tm:$LiNbO_3$ crystal from Gooch & Housego with S2 Corp. internal funds to explore alternate vendors of bulk rare-earth-activated $LiNbO_3$ material.

- Dr. Charles Thiel was asked to give an invited talk at the 47th Winter Colloquium on the Physics of Quantum Electronics in Snowbird Utah, January 8-13, 2017 on our MREDI research and related work.

- Dr. Zeb Barber gave a presentation at a special U. S. Intelligence Advanced Research Projects Activity (IARPA) session of the IEEE Rebooting Computing Conference 2016 in Del Mar, CA on October 19th. This presentation focused on collaborative work by MSU-Spectrum Lab and S2 Corporation on optical computing applications of rare-earth-activated materials. All travel expenses were paid by non-state Spectrum Lab funding.

- Dr. Morgan Hedges from Princeton University visited MSU on August 16, 2016 to discuss ideas for new potential applications of rare-earth-activated materials.

- Dr. Sebastien Ermeneux, Business Manager at AlphaNov Institut d'optique d'Aquitaine, France, visited MSU and several local Montana photonics companies August 24-28, 2016. Dr. Ermeneux gave a presentation at MSU on the business development model employed by AlphaNov to commercialize new technologies and nurture entrepreneurial business startups.

- Prof. Christoph Simon from University of Calgary visited MSU on September 16, 2016 to discuss collaborative research directly related to our MREDI efforts as well as to present a colloquium titled "Quantum optics for quantum networks, fundamental tests, and biology."

- Prof. Andrei Faraon from California Institute of Technology visited MSU on October 7, 2016 to discuss collaborative research directly related to our MREDI efforts as well as to present a colloquium titled "Quantum light-matter interfaces based on rare-earth-doped crystals and nano-photonics."

- Brett Wilkins, who previously worked on this MREDI effort as part of the Cone-Thiel Research Group, has entered the Physics graduate program at MSU while continuing to work at AdvR, Inc..

- Undergraduate student Riley Nerem has joined the Cone-Thiel group to work on MREDI research efforts. His previous research was with IMPACT at CU Boulder, involving extensive use of analog electronics to interface with the accelerator the lab housed.

- Graduate student Tino Woodburn wrote and submitted his doctoral candidacy paper and will give an oral presentation November 1st on "Characterizing and Modifying Optical Properties of Materials Used for Photonic Applications" to complete his candidacy exam.

- Graduate students Aaron Marsh and Tino Woodburn and undergraduate Kyle Olson gave poster presentations on selected aspects of their MREDI work at the annual Optec Optical Science and Laser Technology Conference at MSU on October 4, 2016. The presentations were titles "Theoretical Modeling of Dielectric Strip-Loaded Waveguides," "Characterizing & Designing Rare-Earth-Activated Materials for Photonic Applications," and "Rare-Earth Doped Waveguide Development and Characterization," respectively.

- Graduate student Tino Woodburn presented a poster on “Characterizing & Designing Rare-Earth-Activated Materials for Photonic Applications” at Montana University System Material Science Symposium on October 14. The conference also included talks and discussions involving researchers from the University of Montana, Montana Tech, and Carnegie Mellon University.

Expenditures to date **(**Grant 41W416) Personnel $217,344.06, Benefits $53,266.04, Operations $143,352.59, Capital Equipment $122,200; Total Expenditures **$536,172.69.**

Subproject 9: Optical Parametric Oscillator for Tunable Lasers (Kevin Repasky, repasky@ece.montana.edu, with AdvR, Inc.). Investigate optical parametric oscillator performance in support of characterizing large aperture periodically poled non-linear optical crystals and in support of continued development of large area methane detection.

Milestones

a) December 2016: Model optical parametric oscillator performance using SNLO modeling tools
b) June 30, 2017: Demonstrate singly resonant optical parametric oscillator pumped at 1064 nm and seeded at 1650 nm
c) June 30, 2017: Final report including scientific merit and commercial products or potential

Progress toward objectives

A dither locking system was added to the optical cavity as shown in the block diagram in Figure 9-1. In this process, a sinusoidal signal with a frequency of 5000 Hz from a function generator is fed into an acousto-optic modulator (AOM) that modulates the input seed laser with a Doppler shift. The first order beam is then fiber coupled into the optical amplifier while the rest of the seed laser path remains unchanged. For locking the cavity, the output signal transmitted through the cavity at the seed wavelength of 1571 nm is measured on an InGaAs detector. This information is next sent to the hold circuit and then to the lock-in amplifier. Here, the amplitude of signals oscillating at the dither frequency is extracted to create the error signal which is proportional to the change of cavity length required to keep the cavity in resonant at 1571 nm. This error signal is then used as an input and a reference for a ramp generator when controlling a piezo-electric transducer (PZT) that is attached to the flat mirror for locking the cavity.

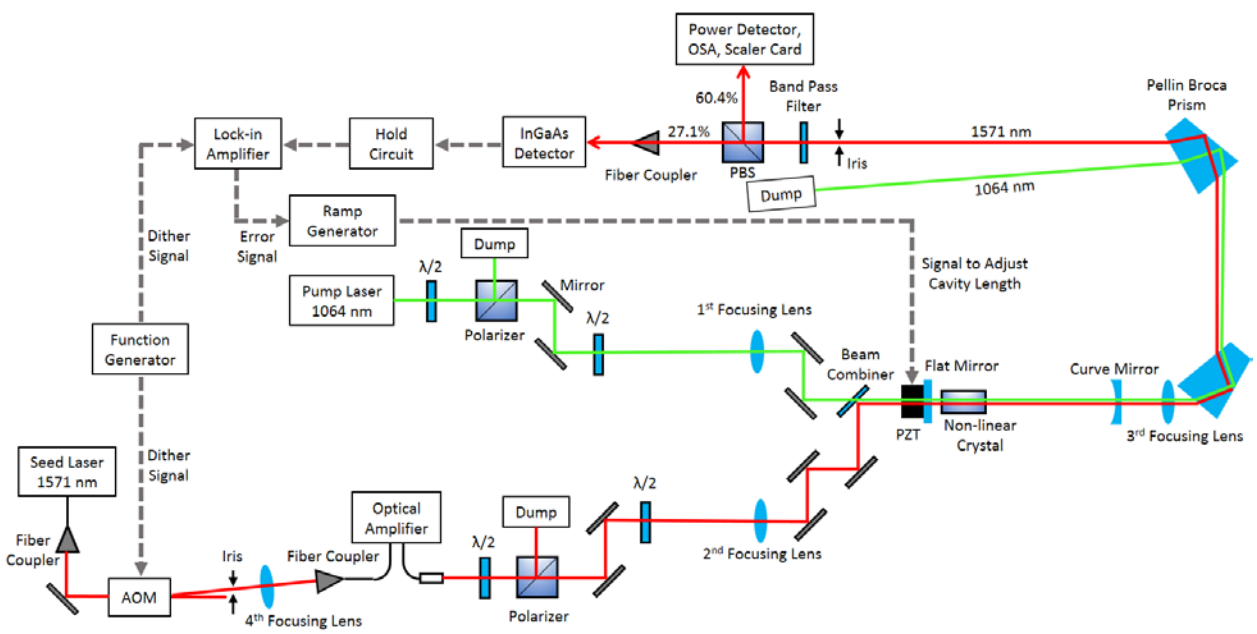

Figure 9-1. Schematic of the setup for the locked OPO

Figure 9-2 shows the results of the output signal energy measurement for OPG, OPA, unseeded-unlocked OPO, seeded-unlocked OPO, and seeded-locked OPO cases. As expected, the output energy from the seeded-locked OPO is the highest among the five, followed by the seeded-unlocked OPO, unseeded-unlocked OPO, OPA, and OPG. At the input pump energy above 8 mJ, all three OPO output energies drops down and becomes lower than that of OPG and OPA. This is likely due to the broadening of the spectra at higher pump energies, which may be corrected with a higher poer seed laser. The conversion efficiency for each case was calculated and plotted in Figure 9-3. The theoretical prediction of both the output energy and the conversion efficiency is currently being analyzed using the SNLO software.

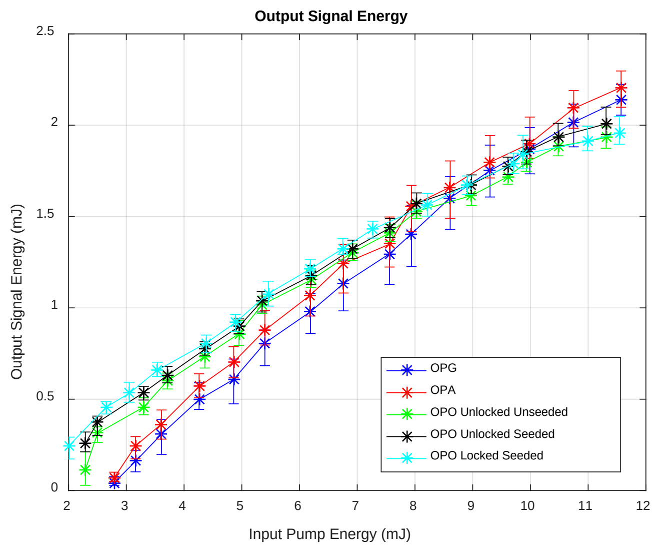

Figure 9-2. Output signal energy for OPG/OPA/OPO cases

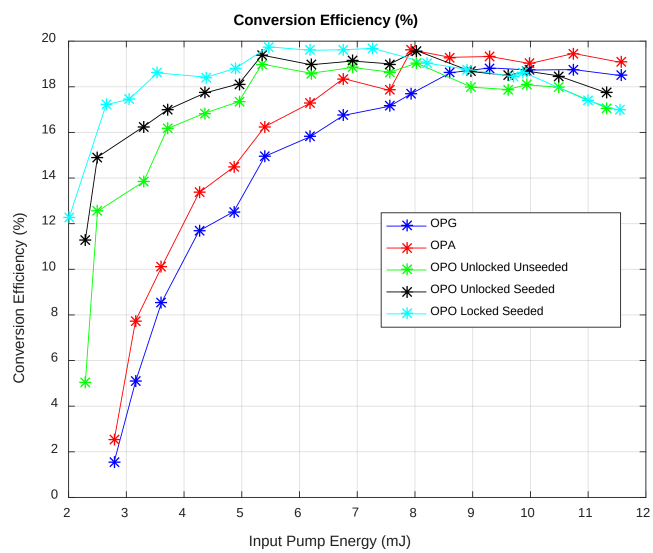

Figure 9-3. Conversion efficiency correspond to figure 9-2.

Output spectra at several input pump energies for all cases are shown in Figures 9-4 through 9-8. The spectra get broader and its peak gets higher when the input pump energy increases.

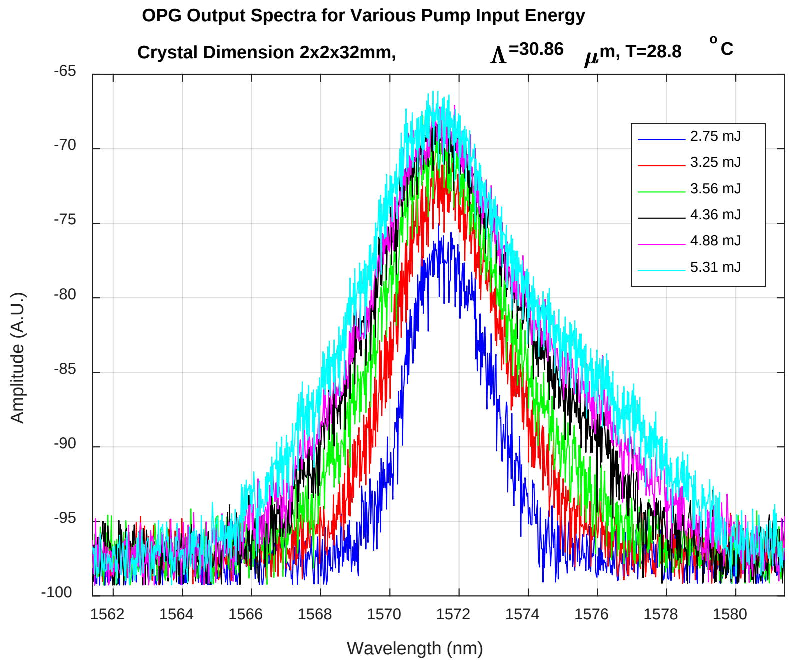

Figure 9-4. Output spectra for OPG.

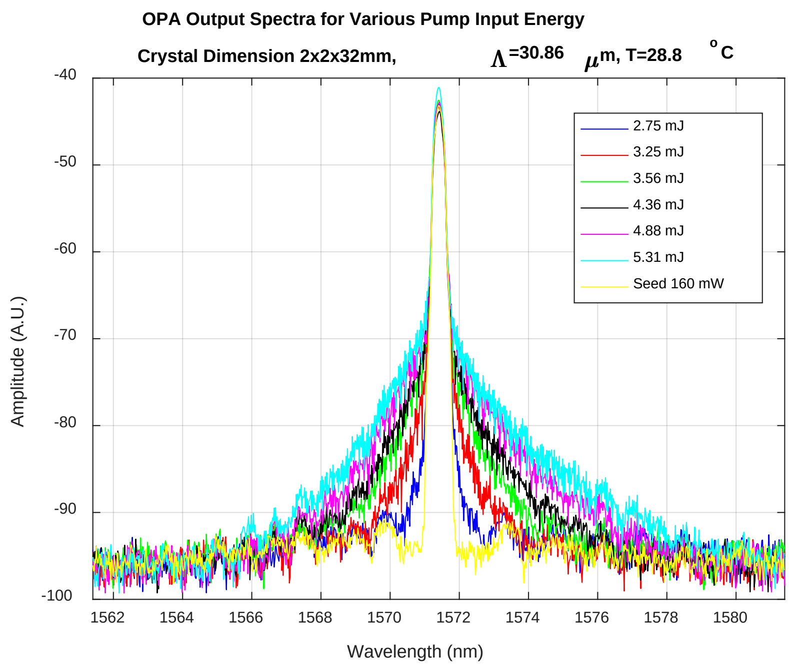

Figure 9-5. Output spectra for OPA.

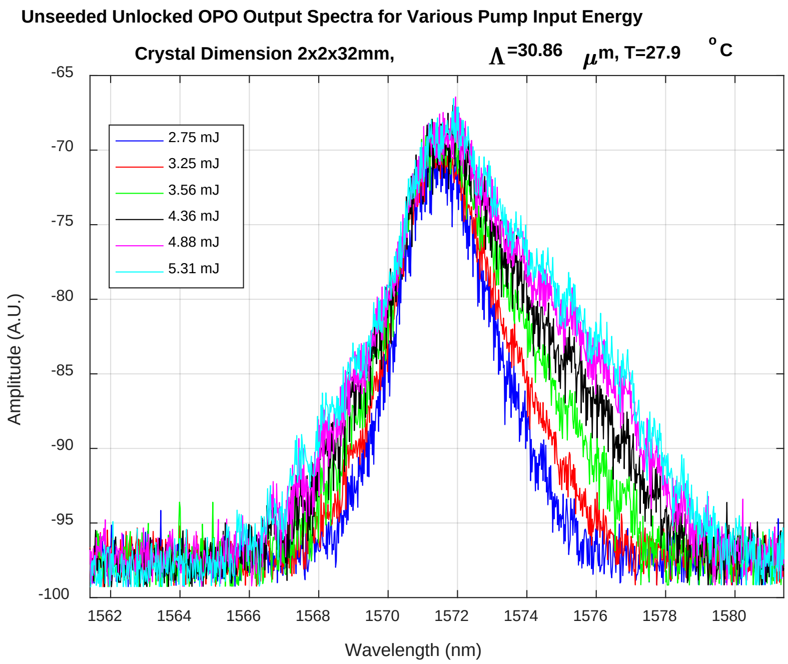

Figure 9-6. Output spectra for unseeded-unlocked OPO.

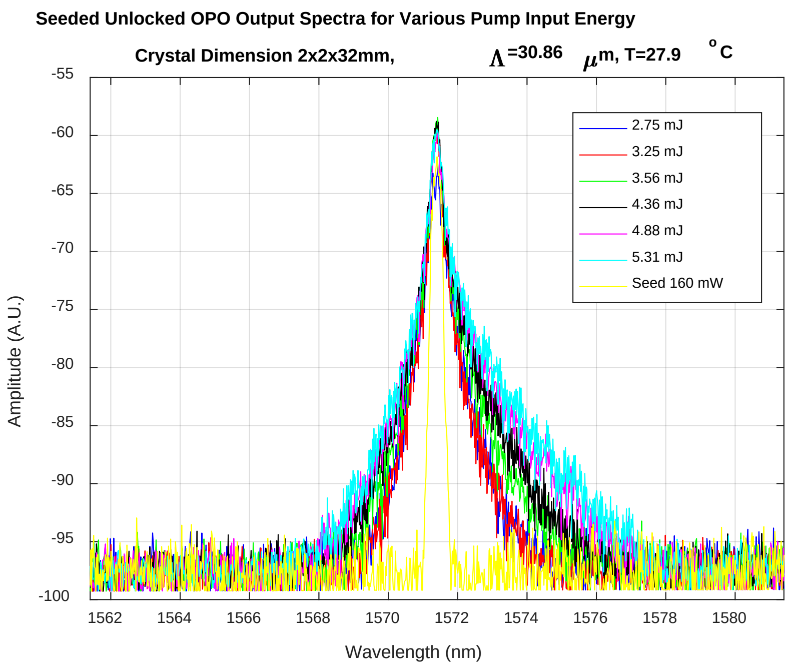

Figure 9-7. Output spectra for seeded-unlocked OPO.

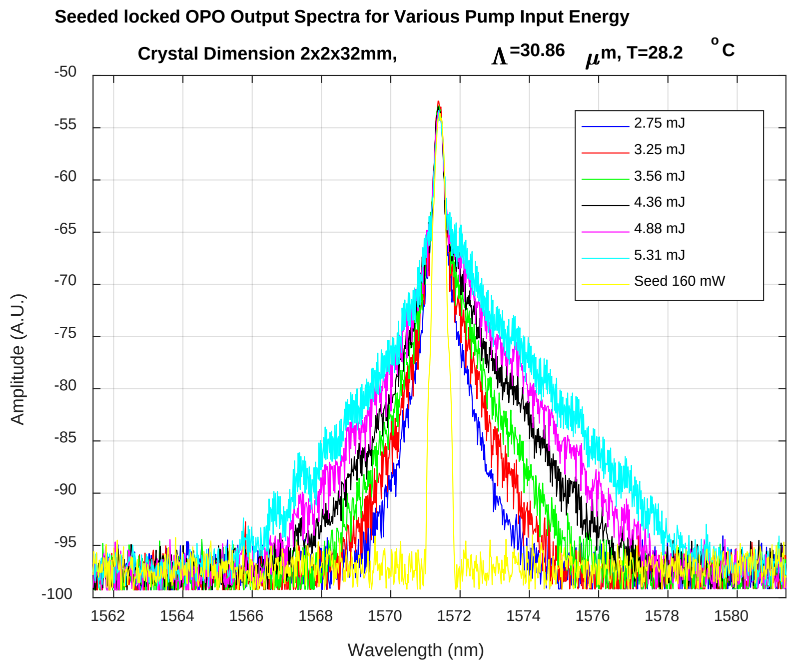

Figure 9-8. Output spectra for seeded-locked OPO.

Figure 9-9 shows the comparison between OPG, OPA, and OPO output spectra for the same input pump energy of 2.75 mJ. All cases demonstrate good spectral overlap because their peaks locate at seed wavelength of 1571.406 nm. Both cases also demonstrate good spatial overlap because the seeded cases have narrower bandwidths than the unseeded cases.

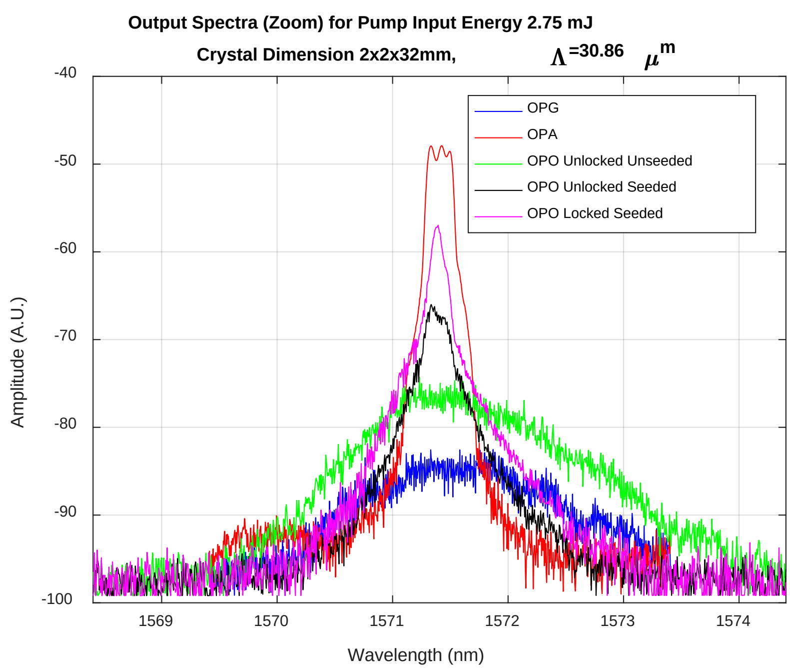

Figure 9-9. Output spectra for OPG/OPA/OPO with 2.75 mJ input pump energy.

The results of the FWHM measurement corresponds to the plot in Figure 9-9 are shown in Table 9-1 and a photograph of the final OPG/OPA/OPO setup is in Figure 9-10.

Table 9-1. FWHM of OPG/OPA/OPO with 2.75 mJ input pump energy.

	FWHM (nm)
OPG	1.4000
OPA	0.2232
Unseeded-unlocked OPO	1.1000
Seeded-unlocked OPO	0.1898
Seeded-locked OPO	0.0941

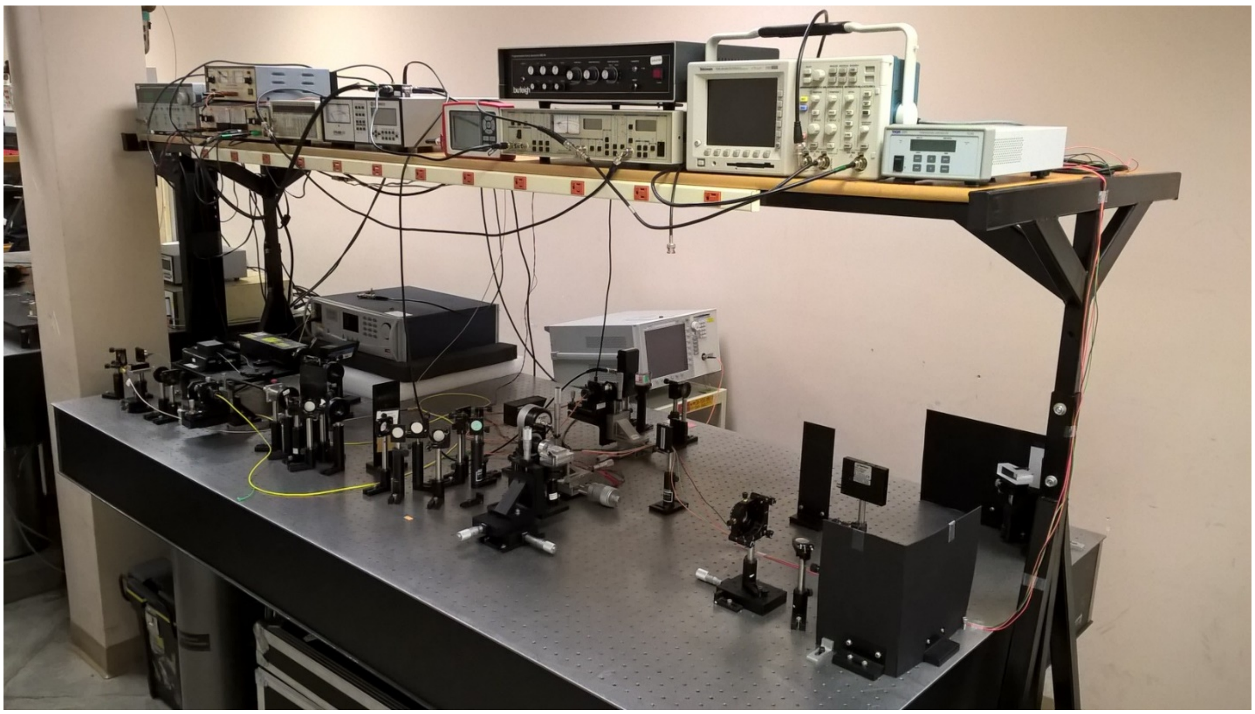

Figure 9-10. The final OPG/OPA/OPO setup.

<u>Expenditures to date</u> (Grant 41W412) Personnel $40,045.55, Benefits $3,273.83, Operations $27,207.90, total Expenditures **$70,527.28**

Subproject 10: Nonlinear Optical Detection of Surface Contaminants (Rob Walker, rawalker@chemistry.montana.edu, with Altos Photonics). Develop a new method for detecting organic contaminants that accumulate on the surface of water based on nonlinear vibrational overtone spectroscopy (NVOS).

Milestones

a) December 2015: Demonstrate feasibility of using new spectroscopic method for surface detection of adsorbed species
b) June 2016: Submit SBIR application with Altos to develop detection and monitoring instrument based on NVOS
c) December 2016: Successful application of NVOS to environmentally relevant systems including contaminants on water surfaces and solid substrates

Progress toward objectives

This project's goal is to develop new surface specific, optical methods capable of detecting adsorbed molecules. Specifically, our efforts are focused on exploiting the advantages of nonlinear optical spectroscopy to create a simple, sensitive technique that can identify the presence of organic contaminants at water/air and solid/liquid interfaces. Our ultimate objective is to use discoveries from our seminal studies to guide the development of portable devices capable of being used for field measurements.

The third quarter of 2016 saw significant disruption and a lack of productivity on this project due to construction for the new dining hall on the north end of CBB. The damage to our Ti:sapphire/OPA amplified laser system was significant in July and early August. Primarily, the damage resulted from concussive shaking that occurred as a steam tunnel was being extended from Willson/Jabs to the new dining hall site. The magnitude of this disruption was documented in the 2nd Quarter report. Visibly, we observed laser spots bouncing by up to 2 mm on optics during this period and laser performance fell by >25%. A second problem posed by construction during the summer months was dust. Despite efforts from the contractors to reduce dust coming into CBB, we observed a significant increase in lab particulate levels (measured with a Dylos particle counter) when construction was taking place. Large amplitude vibrations and poor air quality led to optics burning and/or becoming so badly misaligned that we could not recover performance.

The good news: After working with MSU Safety and Risk Management, the state insurance claims department, and the contractors we were able to successfully file a claim for repair and replacement of damaged parts. The service visit occurred in late October and the optical system is once again performing at a level comparable to early June prior to the start of construction. We are in the middle of realigning optical paths on the table and re-optimizing detector collection efficiency. The process requires ~1 week – 10 days. We expect to be able to acquire meaningful data starting in November.

During this time, we also installed refurbished legs under our optical table so that it now floats. We hope/expect that a floating table will help mitigate and further damage resulting from construction activities as the dining hall foundation is dug and poured.

While students were attempting to cope with the repeated disruptions and accumulating damage during the summer, I submitted one proposal to continue the work initiated with MREDI funding. The proposal was submitted to the Army Research Office following an invitation from a program officer and is entitled:

Organic Enrichment at Environmental Aqueous Interfaces: Cooperative Adsorption and Its Role in Atmospheric Science

The proposal's project summary appears on the next page. The proposal requests $421K ($310K direct) over 3 years with a requested start date of May 1, 2017. If awarded, this proposal will support two graduate students, one of whom will continue to develop new NLO methods for studying interfaces.

A 2nd proposal to be submitted to the NSF was begun in September and was submitted on October 31. This proposal will be described in the next quarterly report.

Organic Enrichment at Environmental Aqueous Interfaces: Cooperative Adsorption and Its Role in Atmospheric Science

Project Summary. Research described in this proposal will test mechanisms thought to be responsible for enhanced organic content in naturally produced aqueous aerosols. Specifically, experiments will identify and quantify the consequences of cooperative adsorption at aqueous-vapor interfaces. In this context *cooperative adsorption* describes accumulation of water-soluble, organic solutes at an aqueous/vapor interface covered with an insoluble Langmuir film. Research will address important, unresolved questions about sea spray aerosols (SSA) composition and the consequences of cooperative adsorption on atmospheric aerosol chemistry. Studies will employ surface specific, nonlinear vibrational spectroscopy coupled with surface tension and ellipsometry measurements to determine interfacial molecular structure and organization as well as adsorption energies and changes in surface optical properties as a function of Langmuir film surface coverage, soluble solute bulk concentration and ionic strength. Specific hypotheses to be tested include:

- *Organic enrichment can be controlled by tuning Coulomb interactions between soluble solutes and adsorbed Langmuir films.* This hypothesis predicts that aqueous pH, ionic strength, and acid/base chemistry will play the primary roles in controlling cooperative adsorption.
- *Cooperative adsorption is concentration dependent.* This hypothesis anticipates that Langmuir films must have a minimum surface coverage before they can enrich soluble solutes at aqueous/vapor interfaces. Also, soluble solutes must have minimum bulk concentrations before they adsorb to Langmuir films.
- *Multivalent interactions between soluble biopolymers and Langmuir films can render cooperative adsorption an irreversible process.* While solution phase monomer adsorption to surfaces may be reversible, we expect that soluble oligomers formed from degraded biomass are more likely to adsorb cooperatively and irreversibly to insoluble Langmuir films.

The proposed research addresses several of the core goals of the ARO's Environmental Sciences Program. These goals include 1) characterizing atmospheric boundary layer processes at high resolution and 2) providing fundamental data that validates the path from observational data to management of atmospheric information. Specifically, this project will examine how solution phase composition, pH and ionic strength affect the surface coverage and adsorption energetics of solutes to aqueous/vapor interfaces covered by insoluble organic films. Experiments will employ systems designed to mimic faithfully those conditions found in ocean environments, but the ability to precisely control variables such as solution phase concentrations, ionic strength and monolayer surface coverage will enable experiments to isolate and quantify adsorption energetics and number densities. More broadly, this work will lead to a clear hierarchy of the noncovalent, intermolecular forces responsible for cooperative adsorption to lipid films and criteria for determining when cooperative adsorption is reversible.

By restricting our studies to carefully chosen systems designed to capture and vary the variables most relevant to ocean surfaces, we expect to be able to isolate the roles played by the insoluble monolayer, soluble solutes and solution conditions. Outcomes from the proposed work will include quantitative thermodynamic data that can be used directly in models that predict interfacial composition and properties of environmental systems where cooperative adsorption enriches interfacial solute concentrations. This information is precisely what is needed to inform and develop models describing SSA properties. Support for this research program will sponsor the Ph.D. research of two graduate students and several undergraduate students.

<u>Expenditures to date</u> (Grant 41W415) Personnel $29,470.26, Benefits $1,745.94, Operations $19,014.70; total Expenditures **$50,230.90**